Advanced Drug Delivery Reviews 64 (2012) 614–628

Contents lists available at SciVerse ScienceDirect

Advanced Drug Delivery Reviews

journal homepage: www.elsevier.com/locate/addr

Intranasal delivery of biologics to the central nervous system ☆

Jeffrey J. Lochhead [a], Robert G. Thorne [a,b,c,d,*]

[a] Pharmaceutical Sciences Division, University of Wisconsin—Madison School of Pharmacy, 5222/5224 Rennebohm Hall, 777 Highland Avenue, Madison, WI 53705, USA
[b] Center for Neuroscience & Neuroscience Training Program, USA
[c] Cellular and Molecular Pathology Graduate Training Program, USA
[d] Clinical Neuroengineering Training Program, University of Wisconsin—Madison, Madison, WI 53706, USA

ARTICLE INFO

Article history:
Received 15 August 2011
Accepted 7 November 2011
Available online 15 November 2011

Keywords:
Drug delivery
Nasal passage
Olfactory
Trigeminal
Proteins
Gene vectors
Stem cells

ABSTRACT

Treatment of central nervous system (CNS) diseases is very difficult due to the blood–brain barrier's (BBB) ability to severely restrict entry of all but small, non-polar compounds. Intranasal administration is a non-invasive method of drug delivery which may bypass the BBB to allow therapeutic substances direct access to the CNS. Intranasal delivery of large molecular weight biologics such as proteins, gene vectors, and stem cells is a potentially useful strategy to treat a variety of diseases/disorders of the CNS including stroke, Parkinson's disease, multiple sclerosis, Alzheimer's disease, epilepsy, and psychiatric disorders. Here we give an overview of relevant nasal anatomy and physiology and discuss the pathways and mechanisms likely involved in drug transport from the nasal epithelium to the CNS. Finally we review both pre-clinical and clinical studies involving intranasal delivery of biologics to the CNS.

Contents

Abbreviations: Aβ, beta amyloid; ANG II, angiotensin II; AVP, arginine vasopressin; BBB, blood–brain barrier; ChAT, choline acetyltransferase; CNS, central nervous system; CSF, cerebrospinal fluid; EPO, erythropoietin; Ex, exendin; GALP, galanin-like peptide; GBC, globose basal cell; HBC, horizontal basal cell; HRP, horseradish peroxidase; IGF-1, insulin-like growth factor-1; INF-β1b, interferon β1b; IN, intranasal; IV, intravenous; MCAO, middle cerebral artery occlusion; MOG, myelin oligodendrocyte protein; MSC, mesenchymal stem cells; MW, molecular weight; NGF, nerve growth factor; OEC, olfactory ensheathing cell; OSN, olfactory sensory neuron; PACAP, pituitary adenylate cyclase-activating polypeptide; siRNA, small interfering RNA; TGF-β1, transforming growth factor β1; TJ, tight junctions; VEGF, vascular endothelial growth factor; V_1, ophthalmic division of trigeminal nerve; V_2, maxillary division of trigeminal nerve; V_3, mandibular division of trigeminal nerve; WGA-HRP, wheat germ agglutinin-horseradish peroxidase; ZO, zonula occludens.

☆ This review is part of the *Advanced Drug Delivery Reviews* theme issue on "Delivery of Therapeutics to the Central Nervous System".

* Corresponding author at: Pharmaceutical Sciences Division, University of Wisconsin—Madison School of Pharmacy, 5113 Rennebohm Hall, 777 Highland Avenue, Madison, WI 53705-2222, USA. Tel.: +1 608 890 3508.
E-mail address: rthorne@wisc.edu (R.G. Thorne).

0169-409X/$ – see front matter
doi:10.1016/j.addr.2011.11.002

1. Introduction

The blood–brain barrier (BBB) is located at the level of the cerebral microvasculature and is critical for maintaining central nervous system (CNS) homeostasis. Although the BBB restricts the entry of potentially neurotoxic substances into the brain, it also presents a major obstacle to the delivery of therapeutics into the CNS for disease treatment. The BBB exhibits a low rate of pinocytosis and possesses tight junctions (TJ) which form a seal between opposing endothelial membranes [1]. The presence of TJ at the BBB creates a high transendothelial electrical resistance of 1500–2000 Ω·cm^2 compared to 3–30 Ω·cm^2 across most peripheral microvessels [2,3]. This high resistance is associated with very low permeability, i.e. the BBB greatly restricts paracellular diffusion of solutes from the blood into the brain. Typically, only small, lipophilic molecules appreciably cross the normal, healthy BBB via transcellular passive diffusion, although some limited transport of certain peptides and peptide analogs has been reported [4]. Essential nutrients such as glucose or iron gain entry into the CNS through specific transporters such as the glucose transporter 1 or receptors such as the transferrin receptor [5,6]. Receptors and transporters for gastrointestinal hormones involved in regulating metabolism are expressed at the BBB in order to convey information between the CNS and periphery [7]. In addition to its low paracellular permeability and low rate of pinocytosis, the BBB also expresses a high number of drug transporters (e.g. P-glycoprotein) which further restrict brain entry of many endogenous and exogenous substances that would otherwise be predicted to cross the BBB based on molecular weight (MW) and lipophilicity considerations [8,9].

Although there are many examples of small MW drugs which cross the BBB, nearly all large MW substances are severely restricted from crossing the BBB under normal conditions; indeed, the only examples of large MW drugs approved for clinical use in treating a neurological illness are those that act via peripheral mechanisms (e.g. type I interferons for treating multiple sclerosis). Many large MW substances have shown substantial promise in treating aspects of CNS diseases based on studies utilizing in vitro systems and animal models. However, it will likely be necessary to implement drug delivery strategies that overcome the formidable obstacles presented by the various barriers of the CNS (the BBB and blood–cerebrospinal fluid (CSF) barriers) for these studies to ultimately be translated to the clinic [10]. Intraparenchymal, intracerebroventricular, and intrathecal injections/infusions are capable of delivering therapeutics directly to the CNS, but these routes of administration are invasive and likely not practical for drugs which need to be given chronically. The intranasal (IN) route of administration provides a non-invasive method of bypassing the BBB to potentially deliver biologics such as peptides, proteins, oligonucleotides, viral vectors, and even stem cells to the CNS. The IN route has long been associated with a number of advantages (Table 1), e.g. rapid onset of effects using non-injectable administration methods and a growing record of experience with approved formulations (e.g. nasal spray of the 3.5 kDa polypeptide hormone calcitonin has been used for many years to treat postmenopausal osteoporosis); the major disadvantage of the route (Table 1), aside from the challenge of reproducibility, is that limited absorption across the nasal epithelium has restricted its application to particularly potent substances, although this can be overcome by use of permeation enhancers in some cases [11]. While nasal delivery has probably been the most successful of the alternative transmucosal routes as a portal of entry into the systemic circulation for substances that cannot be given orally [12], with a large number of intranasally applied drugs in clinical use [11], research into whether the IN route might deliver potentially therapeutic amounts of larger biologics such as proteins to the CNS was first described only a little over a decade ago [13,14]. Delivery of biologics and a variety of other substances from the nasal passages to the brain has now been documented in numerous animal and clinical studies [15–17]. Here we will provide an overview of relevant nasal anatomy and physiology and discuss the pathways and transport mechanisms that may be involved in the distribution of biologics from the nasal cavity to the CNS. We will also summarize the findings of key studies that convincingly show entry and/or efficacy of biologic drugs introduced to the CNS using the intranasal route of administration.

2. Nasal anatomy

2.1. General considerations

The nasal cavity extends from the nostrils (nares) to the nasopharynx and is divided longitudinally by the nasal septum [18]. The human nasal cavity only extends approximately 12–14 cm in length yet has a large absorptive surface area of ~160 cm^2 due to three bony structures called turbinates or conchae (inferior, middle and superior) which also aid in filtering, humidifying and warming inspired air [18]. Tables 2 and 3 summarize important comparative aspects of nasal anatomy with respect to humans, monkeys and rats, three of the most commonly used species in studies evaluating systemic absorption and brain targeting following intranasal administration. Several differences in the nasal anatomy and physiology of rats and primates are notable [19]. Primates are oronasal breathers while rats are obligate nasal breathers and rely more heavily on their keen sense of smell. The architecture of the rat nasal passage is generally more complex than that of the primates, with a significantly higher surface area-to-volume ratio. Importantly, mucociliary clearance (propulsion of mucus on the surface of the nasal epithelium by

Table 1
Advantages and disadvantages of intranasal drug delivery.

Advantages	Disadvantages
Non-invasive/reduced infection risk from application/low risk of disease transmission	Limited to potent drugs/small volumes (25–200 μl)
Ease of self-administration/dose adjustment	Active mucociliary clearance
Large surface area for absorption (human ~160 cm^2)	Enzymatic degradation by nasal cytochrome P450/peptidases/proteases (pseudo first-pass effect)
Rapid absorption/fast onset of action	Low permeability for hydrophilic drugs without absorption enhancers necessitates large doses
Rich, vascular submucosa and lymphatic system	Low pH of nasal epithelium
Avoid hepatic first-pass elimination	Interindividual variability
Possible direct pathways to the CNS bypassing the blood–brain barrier	Low CNS delivery efficiencies for proteins measured thus far (<0.05%)

Table 2
Qualitative similarities and differences in the nose and upper airways between humans, monkeys and rats [19,156,157].

	Human	Monkey	Rat
Shape of upper airways	L-shaped	L-shaped	Linear
Type of breathing at rest	Oronasal	Oronasal	Obligatory nose
Connection between nasal cavity and oral cavity	No (incisive canal is not patent)	No (incisive canal is not patent)	Yes (nasopalatine canal is patent)
Vascular swell bodies in septum	No	No	Yes
Turbinates (number and shape)	3; comma-shaped	3; comma-shaped	3; t-shaped with elaborate scrolls
Presence of ethmoid sinuses (air cells) & sphenoid sinuses	Yes	No	No
Maxillary sinuses	Large; Open	Large; Open	Small; Closed
Nasal secretion movement	Mostly posteriorly (to nasopharynx)	Mostly posteriorly (to nasopharynx)	Mostly anteriorly (towards nostril)
Inspiratory airflow route	Close to floor of nasal passage	Close to floor of nasal passage; vortex in vestibule	Upward and laterally

respiratory mucosal cilia) is directed mostly anteriorly in rats while in primates nasal secretions are mostly transported posteriorly toward the nasopharynx. Finally, macrosmatic species such as the rat have a significantly higher percentage of nasal epithelium devoted to olfaction (the sense of smell) compared to microsmotic species such as humans and monkeys. Nevertheless, studies in rats are critically important and have been used to establish much of what we know about the pathways and mechanisms underlying nasal delivery to both the systemic circulation and the CNS simply because it is far less practical to conduct certain types of research in primate species.

There are four types of epithelia in the nasal cavity: squamous, respiratory, transitional, and olfactory [18]. The nasal vestibule, extending from just inside the nares to the anterior portion of the inferior turbinates, is lined with stratified squamous epithelium which contains coarse hairs in addition to sebaceous and sweat glands. The transitional epithelium is a non-ciliated cuboidal or columnar epithelium located between the squamous and respiratory epithelia and the respiratory and olfactory epithelia. We will focus our attention on the olfactory and respiratory epithelia because they represent the most likely sites of absorption for drugs administered intranasally.

2.2. Olfactory region

The olfactory region comprises <10% of the surface area of the nasal epithelium in man. It consists of a pseudostratified columnar epithelium located on the most superior aspect of the nasal cavity that is responsible for mediating the sense of smell. Olfactory sensory neurons (OSN) have several unique attributes: they are the only first order neurons possessing cell bodies located in a distal epithelium and the tips of their dendritic processes, which end as enlarged knobs with several non-motile cilia, extend far into the overlying mucus layer that is directly exposed to the external environment (Fig. 1A and B). The OSN are bipolar cells possessing odorant-responsive receptors in the plasma membrane of the olfactory cilia; easy access of odorants to OSN receptors in the mucus lining the olfactory epithelium is essential to the process of olfaction. The unmyelinated axons of OSN extend through the epithelial basal lamina and converge with axons from other OSN to form nerve bundles called fila olfactoria. Interlocking olfactory ensheathing cells (OEC) enclose the fila olfactoria in continuous channels from their origin to the olfactory bulb. The olfactory ensheathing cells are further enclosed by multicellular sheets of olfactory nerve fibroblasts to form a perineural-like sheath around the fila olfactoria [20]. The ensheathed fila olfactoria comprise the olfactory nerve and travel through the cribriform plate of the ethmoid bone into the brain where they terminate on dendrites of the mitral, periglomerular, and tufted cells in glomeruli of the olfactory bulb. Olfactory information is then sent through axons of the mitral and tufted cells to a number of areas including the anterior olfactory nucleus, olfactory tubercle, piriform cortex, amygdala and entorhinal cortex [21].

Several other types of cells reside in the olfactory epithelium in addition to OSN. Sustentacular cells extend from the apical region of the epithelium to the basal lamina and act as supporting cells [22]. They possess long, irregular microvilli which intermingle with the cilia of the OSN. Cells of the Bowman's gland form tubular-type ducts which originate in the lamina propria and traverse the basal lamina to produce and secrete a serous fluid which acts as a solvent for odor molecules. There are also horizontal basal cells (HBC) and globose basal cells (GBC). The HBC are located along the basal lamina and act as multipotent progenitors to GBC, sustentacular cells and cells of the Bowman's gland and duct [23]. The GBC are located slightly higher than the HBC in the olfactory epithelium and act as neural progenitors, providing a source for continual OSN replacement [24]. Small populations of cells lined with numerous microvilli also exist in the olfactory epithelium. These cells are referred to as microvillus cells and have an unknown function [25]. Blood vessels, inflammatory cells, and lymphatic vessels which drain into the deep cervical lymph nodes in the neck are also present in the submucosa (lamina propria) of the olfactory region.

Table 3
Quantitative morphometric data for the nasal passages of humans, monkeys and rats [19,156,157].

	Human	Rhesus monkey	Rat
Body weight	70 kg	7 kg	0.25 kg
Nasal cavity volume (V)	25 cm^3	8 cm^3	0.26 cm^3
Nasal cavity surface area (SA)	160 cm^2	62 cm^2	13.4 cm^2
Surface area per unit volume (relative surface area; SA/V)	6.4	7.75	51.5
Olfactory epithelium (area; %)	12.5 cm^2; 8%	6–9 cm^2; 10–15%	6.75 cm^2; 50%

2.3. Respiratory region

The nasal respiratory epithelium lines approximately 50% of the nasal cavity in rats and 80–90% in humans. It is a pseudostratified columnar secretory epithelium (Fig. 2A) which warms and humidifies inspired air in addition to removing particulates, microorganisms, and allergens. The human respiratory epithelium is comprised of goblet cells, ciliated cells, intermediate cells, and basal cells [26]. Serous glands, seromucous glands, and intraepithelial glands are also associated with the nasal respiratory epithelium. The seromucous glands are responsible for producing most nasal secretions while the goblet cells also secrete mucus [27]. The primary role of the ciliated cells is to use their motile cilia, immersed in periciliary fluid, to propel mucus towards the nasopharynx where it is either swallowed or expectorated. Basal cells function as progenitors to the other cell types in the nasal respiratory epithelium. Importantly, the nasal respiratory epithelium is innervated by branches of the trigeminal nerve [28]; fibers from trigeminal ganglion cells ramify extensively within the nasal mucosa, with many extending almost completely

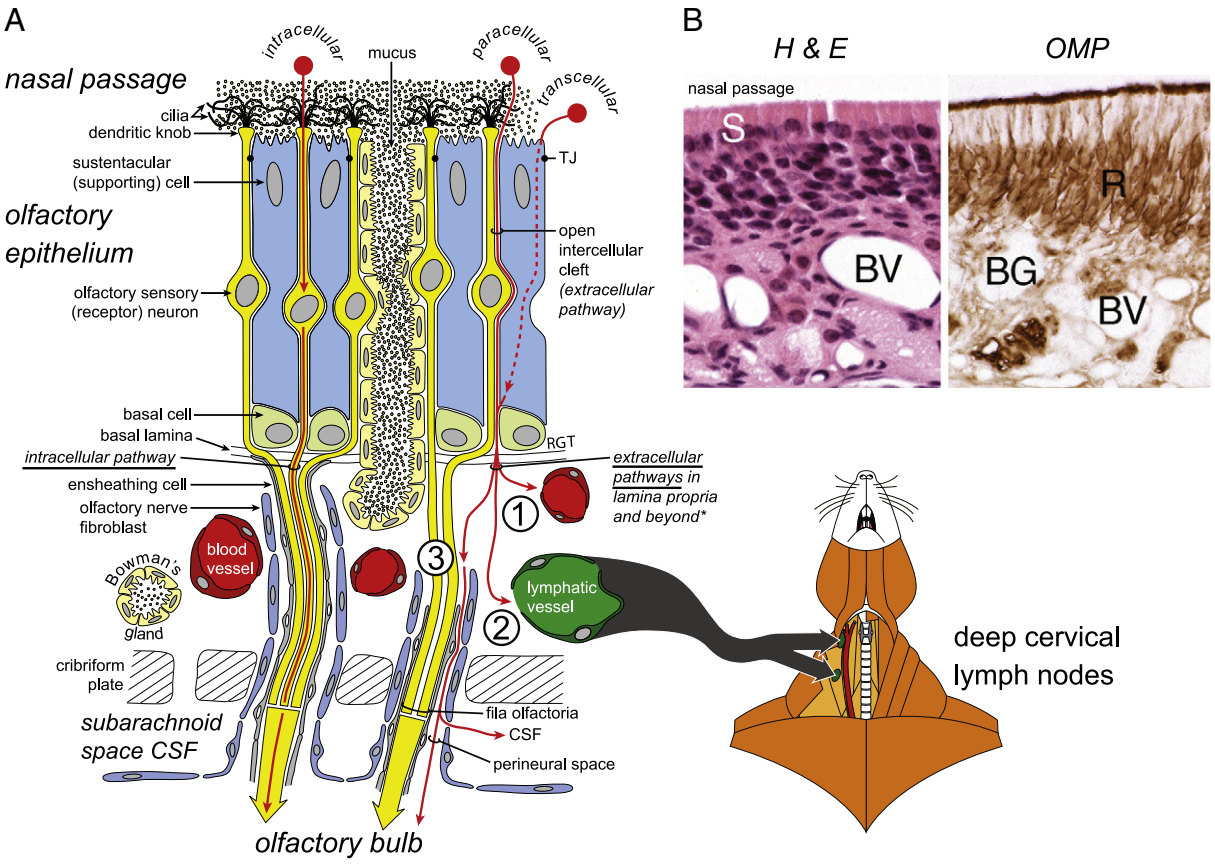

Fig. 1. General organization of the olfactory region. (A) The olfactory mucosa includes the olfactory epithelium and its underlying lamina propria. Axonal processes of olfactory sensory neurons converge into bundles (fila olfactoria), surrounded by ensheathing cells and fibroblasts, before projecting to the olfactory bulb. Potential pathways for drug delivery across the olfactory epithelium following intranasal administration are shown in red. Some substances may be transported by an *intracellular* pathway from the olfactory epithelium to the olfactory bulb within olfactory sensory neurons following adsorptive, receptor-mediated or non-specific fluid phase endocytosis. Other substances may cross the olfactory epithelial barrier by *paracellular* or *transcellular* transport to reach the lamina propria, where a number of different *extracellular* pathways for distribution are possible, as indicated: (1) absorption into olfactory blood vessels and entry into the general circulation; (2) absorption into olfactory lymphatic vessels draining to the deep cervical lymph nodes of the neck; and (3) extracellular diffusion or convection in compartments associated with olfactory nerve bundles and entry into the cranial compartment. Transport within the perineural space bounded by olfactory nerve fibroblasts is indicated but other possibilities exist, e.g. transport within the fila olfactoria compartment contained by ensheathing cells, transport within the perivascular spaces of blood vessels traversing the cribriform plate with olfactory nerves (not shown) or transport within lymphatics traversing the cribriform plate with olfactory nerves (not shown). Possible pathways for distribution of substances from the perineural space into the olfactory subarachnoid space cerebrospinal fluid (CSF) or into the olfactory bulb are shown. (B) Sections through the rodent olfactory mucosa stained with hematoxylin and eosin (H & E) or immunostained using an antibody to olfactory marker protein (OMP), a protein present only in mature olfactory sensory neurons and not sustentacular or basal cells. The sections show the layers of the olfactory epithelium, positions of the sustentacular (S) cells, olfactory sensory (receptor, R) neurons and the numerous blood vessels (BV) and Bowman's glands (BG) within the lamina propria. (Images of sections courtesy of Professor Harriet Baker, Weill Medical College of Cornell University.)

through the epithelium (both respiratory and olfactory) so that their free nerve endings lie very near the epithelial surface (stopping at the TJ level) [29].

The trigeminal nerve, or the fifth (V) cranial nerve, is the largest of the twelve cranial nerves and its distribution and nasal passage innervation are well understood (Fig. 2B) [28,30,31]. The trigeminal nerve exits the pons laterally and consists of a very large sensory root and a small motor root. It is therefore referred to as a mixed nerve, carrying motor fibers to the muscles of mastication and transmitting sensory information from the face, scalp, mouth and nasal passages. The trigeminal nerve runs underneath the dura as it courses rostrally. The three major branches of the trigeminal nerve include the ophthalmic nerve (V_1), the maxillary nerve (V_2), and the mandibular nerve (V_3); the trigeminal nerve is mostly composed of somatic afferent fibers, i.e. sensory information is being conveyed *into* the brain from the nasal passages and other innervated areas. V_1 and V_2 are sensory nerves that also carry autonomic fibers. V_3 contains the mixed portion of the trigeminal nerve, as it is joined by the trigeminal motor root which merges with V_3 after passing underneath the semilunar (trigeminal) ganglion. In humans, V_1 enters the cranial compartment through the superior orbital fissure, V_2 enters the cranial compartment through the foramen rotundum, and V_3 enters the cranial compartment through the foramen ovale. In rats, V_1 and V_2 enter the cranial compartment through the anterior lacerated foramen while V_3 again enters through the foramen ovale. Ethmoidal (V_1), nasopalatine (V_2) and nasal (V_2) branches of the trigeminal nerve provide sensory innervation to the nasal passages [30,32]. The trigeminal sensory nerves project to trigeminal nuclei located in different positions within the brainstem and spinal cord. A portion of trigeminal ganglion cells with sensory endings located in the nasal epithelium also send collaterals directly into the olfactory bulb in addition to the brainstem [33]. The trigeminal motor nucleus, located in the upper pons, contains the nuclei of motor neurons that travel in the small motor root to the muscles of mastication. The remaining three trigeminal nuclei mediate aspects of sensation. Of these, the principal sensory nucleus is located in the pons, lateral to the motor nucleus, the mesencephalic trigeminal nucleus reaches from the upper pons to the midbrain and the spinal trigeminal nucleus extends from the medulla down into the upper cervical spinal cord. Other nerves located in the nasal passages include the nervus terminalus (terminal nerve; cranial nerve zero) and the vomeronasal nerve and organ (Jacobsen's organ) although

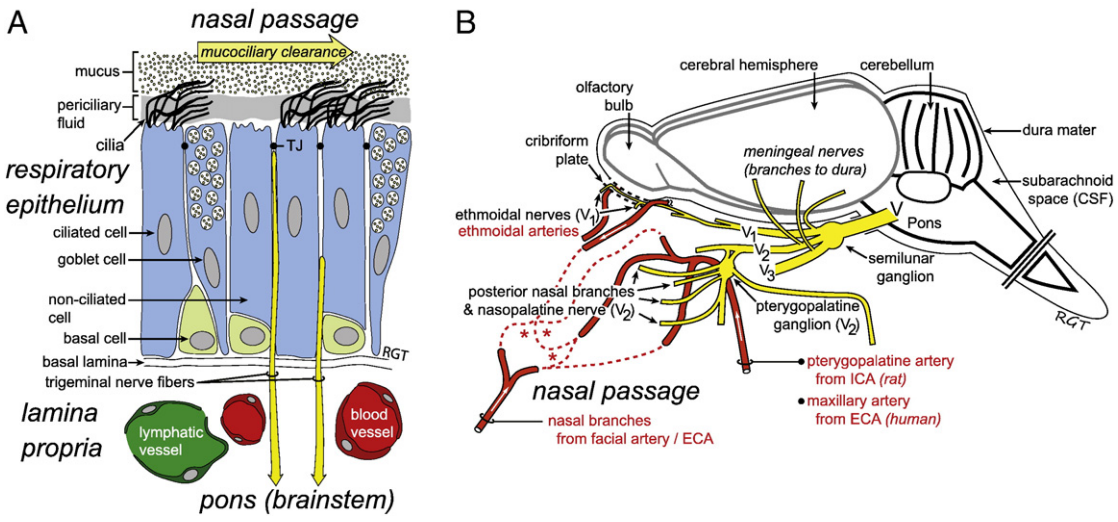

Fig. 2. General organization, trigeminal innervation and vasculature of the nasal respiratory region. (A) The respiratory mucosa includes the respiratory epithelium and its underlying lamina propria. Fibers of the trigeminal nerve, important for conveying chemosensory, nociceptive, touch, and temperature information, are found throughout the nasal epithelium where their free nerve endings extend nearly to the epithelial surface, just beneath tight junctions (TJ). (B) Central projections of the trigeminal nerve shown together with the vasculature of the nasal passage. The cell bodies of the trigeminal nerve fibers are located in the semilunar ganglion; their axons project into the brainstem at the level of the pons where they ultimately synapse with neurons in brainstem areas such as the principal sensory and spinal trigeminal nuclei. Of the three main trigeminal nerve divisions (V_1, the ophthalmic nerve; V_2, the maxillary nerve; and V_3, the mandibular nerve), only V_1 and V_2 send branches to the nasal epithelium. Blood supply to the nasal passages is provided by ethmoidal branches of the ophthalmic artery, sphenopalatine branches of either the external carotid artery (ECA)/maxillary artery (in humans) or the internal carotid artery (ICA)/pterygopalatine artery (in rats), and nasal branches from the ECA/facial artery. Numerous anastomoses (*) connect these branches within the nasal passages.

neither nerve has yet been implicated as providing a pathway for CNS drug delivery.

2.4. Vasculature of the nasal passages

The nasal passages are highly vascular, an important feature mediating the absorption of many drugs into the systemic circulation. Blood supply to the nasal passages [28,34,35] is principally provided by (i) branches of the ophthalmic artery: the anterior and posterior ethmoidal arteries (olfactory region, anterior septum, and anterior lateral wall), (ii) the sphenopalatine artery (mostly posterior septum and posterior lateral wall with smaller branches extending to further areas) and (iii) branches of the facial artery (antero-inferior septum and lateral wall); extensive anastomoses occur between each of these arteries in the antero-inferior portion of the septum known in humans as Kiesselbach's plexus (Little's area), a common site for nose bleeds. Notable species differences exist between rats and humans in the arteries upstream of the ophthalmic and sphenopalatine arteries. In humans, the ophthalmic artery branches directly from the internal carotid artery, while in rats the ophthalmic artery arises from the pterygopalatine artery (rudimentary in humans). The sphenopalatine artery in humans is a branch of the maxillary artery (external carotid artery), while in rats the sphenopalatine artery arises from the pterygopalatine artery (internal carotid artery). Venous drainage from the nasal passages of humans occurs principally through the sphenopalatine vein (posterior nasal passage) and veins accompanying the ethmoidal arteries (anterior nasal passage); some veins pass through the cribriform plate, joining others on the frontal lobe [34].

3. Pathways from the nasal passages to the central nervous system

The precise pathways and mechanisms by which a drug travels from the nasal epithelium to various regions of the CNS have not been fully elucidated. The central distribution of [^{125}I]-labeled proteins following IN administration in rats and monkeys has suggested that delivery occurs along olfactory and trigeminal nerve components in the nasal epithelium to the olfactory bulb and brainstem, respectively, with further dispersion to other CNS areas from these initial points of brain entry [36,37]. At least three sequential transport steps are therefore necessary for a substance to be delivered to distant, widespread sites within the CNS following IN administration: (1) transport across the epithelial 'barriers' (olfactory or respiratory) in the nasal passages, (2) transport from the nasal mucosa to sites of brain entry near the pial brain surface in the cranial compartment (i.e. entry points of peripheral olfactory or trigeminal nerve-associated components comprising the delivery pathways) and (3) transport from these initial brain entry sites to other sites within the CNS.

3.1. Transport across nasal epithelial barriers

Transport across the 'barriers' presented by the olfactory or respiratory epithelia may occur either by *intracellular* or *extracellular* pathways. Intracellular pathways across the olfactory epithelium include endocytosis into OSN and subsequent intraneuronal transport to the olfactory bulb or transcytosis (i.e. transcellular transport) across sustentacular cells to the lamina propria as shown in Fig. 1A. OSN have the ability to endocytose certain viruses (e.g. herpes, poliomyelitis, rhabdoviruses) as well as large molecules such as horseradish peroxidase (HRP), wheat germ agglutinin-horseradish peroxidase (WGA-HRP) and albumin from the nasal passages and then transport them intracellularly along the axon in the anterograde direction towards the olfactory bulb [13,38–42]. HRP is taken up by OSN to a limited extent via fluid-phase endocytosis whereas WGA-HRP is internalized by OSN more avidly via adsorptive endocytosis [40]. Intracellular pathways across the respiratory epithelium potentially include endocytosis into peripheral trigeminal nerve processes located near the epithelial surface and subsequent intracellular transport to the brainstem or transcytosis across other cells of the respiratory epithelium to the lamina propria (see Fig. 2A for relationships). Similar to what is observed in OSN, IN WGA-HRP is internalized and transported intraneuronally within the trigeminal nerve to the brainstem [43,44]. Viruses and bacteria may also be transmitted to the CNS along trigeminal nerve components within the nasal passages [44,45].

Extracellular transport pathways across either the olfactory or respiratory epithelia primarily include paracellular diffusion to the underlying lamina propria (e.g. as shown in Fig. 1A for the olfactory

epithelium). In addition to its intracellular uptake by OSN, HRP has been shown to pass through open intercellular clefts to reach the olfactory bulb when applied intranasally in mice and squirrel monkeys [46]. Electrical resistance measurements across excised rabbit nasal epithelium have yielded values ranging from 40 $\Omega \cdot cm^2$ [47], suggesting relatively permeable barrier properties, to 261 $\Omega \cdot cm^2$ [48], suggesting tightness comparable to the intestinal epithelium. The presence of TJ at an epithelial barrier will be the primary determinant of a given molecule's paracellular permeability. Significantly, the TJ proteins zonula occludens (ZO)-1, 2 and 3, occludin, and claudins-1, 3, 4, 5 and 19 are all expressed in the olfactory epithelium of rats [49,50]. Studies utilizing electron microscopy have shown that TJ exist between nasal epithelial cells but questions remain as to their tightness, continuity and permeability to tracers [51,52]. It has been suggested that the regular turnover of cells in the nasal epithelium may lead to continual rearrangement and loosening of the TJ [51], a consequence of resident basal cell populations dividing throughout life to replace OSN/sustentacular cells in the olfactory epithelium and ciliated/goblet cells in the respiratory epithelium. In the intestine, colloidal gold nanoparticles have been shown to cross the epithelium and distribute to other tissues through large transepithelial spaces created by degrading enterocytes in a process known as persorption [53]. Although speculative, the replacement of cells throughout life may create similar potential spaces in both the olfactory and respiratory epithelia of the nasal passages, possibly facilitating paracellular transport of larger MW substances to the lamina propria.

3.2. Transport from the nasal mucosa to sites of brain entry

Transport from the nasal mucosa to brain entry points at the level of the olfactory bulbs or brainstem may in theory occur via *intracellular* pathways (endocytosis and intraneuronal transport within OSN or trigeminal ganglion cells) or *extracellular* pathways (diffusion or convection within perineural, perivascular or lymphatic channels associated with olfactory and trigeminal nerve bundles extending from the lamina propria to the brain). Intracellular pathways have been covered above in Section 3.1. The possible fates of substances reaching the extracellular environment of the lamina propria are numerous and include: (1) absorption into blood vessels and entry into the general circulation; (2) absorption into lymphatic vessels draining to the deep cervical lymph nodes of the neck; (3) extracellular diffusion or convection in compartments associated with nerve bundles, particularly perineural or perivascular spaces, with subsequent entry into the cranial compartment (Fig. 1A).

Once a substance crosses the nasal epithelium into the lamina propria, it may be absorbed by the rich supply of nasal blood vessels and enter the systemic circulation. Drugs absorbed into the systemic circulation would then have to cross the BBB or blood–CSF barriers to reach the CNS. The nasal vasculature may therefore act as a sink for some IN applied substances, effectively preventing them from reaching the CNS. Although some nasal endothelial cells express TJ proteins such as ZO-1, occludin, and claudin-5, large capillaries of the lamina propria as well as smaller capillaries surrounding glands in the nasal respiratory epithelium possess fenestrations with porous basement membranes [49,54]. Nasal venules and arterioles are continuous and lack fenestrations. It has been reported that blood vessels in the lamina propria of the olfactory submucosa appear permeable to both lanthanum nitrate (MW = 139 Da) and Evans blue (MW = 961 Da) [49]. Following Evans blue injection into the tail vein of rats, both the respiratory and olfactory regions were stained green–blue (respiratory > olfactory) while the olfactory bulb and cortex were unstained. The vasculature in tissue stained following intravenous (IV) injection of Evans blue is often interpreted to be permeable to molecules > 67 kDa because Evans blue has a high affinity for serum albumin (MW = 66.7 kDa). However, non-negligible fractions of free Evans blue as well as Evans blue bound to non-albumin proteins also exist in the serum, complicating interpretation of Evans blue staining following IV injection [55]. Nevertheless, the observation that the olfactory and respiratory regions of the nasal cavity are stained following IV Evans blue while the brain is not demonstrates that the blood vessels in the nasal mucosa are more permeable than cerebral vessels comprising the BBB.

In the nasal submucosa, substances that aren't absorbed into the bloodstream may drain to the deep cervical lymph nodes through nasal lymphatic vessels in the lamina propria. Many dyes and proteins administered intranasally may be recovered at least in part from the deep cervical lymph nodes in the neck [56,57]. It has been known for well over 100 years that dyes injected into the CSF of the subarachnoid space will stain the perineural space of the olfactory nerve and drain through the nasal mucosa into the deep cervical lymph nodes [58]. Large MW compounds such as Evans blue-albumin or [^{125}I]-albumin are concentrated in the perivascular spaces of the middle cerebral arteries and in the deep cervical lymph nodes after injection into CSF or brain [59]. When the cribriform plate is sealed by injection of kaolin or acrylate glue the lymphatic drainage of [^{125}I]-albumin following intraventricular infusion is significantly reduced [59]. Microfil injections into the CSF compartment of human cadavers also show evidence of connections between CSF and nasal lymphatic vessels [60]. These studies suggest that the subarachnoid space, nasal mucosa, and deep cervical lymph nodes are in potential communication with each other for at least some substances.

Substances which have crossed the nasal epithelium to reach the lamina propria but escape local absorption into the blood stream and drainage within nasal lymphatics to the deep cervical lymph nodes may be available to enter the CNS. Faber showed in 1937 that potassium ferrocyanide and iron ammonium citrate solutions applied to the rabbit nasal cavity can be subsequently found in the spaces of the perineural sheath surrounding the olfactory nerve, suggesting that some direct pathways from the nasal passages to the brain may be similar to pathways in the reverse direction [58]. A more recent study obtained a similar perineural distribution of fluorescently labeled 3 kDa dextran around olfactory nerve bundles in both the lamina propria and the outermost layer of the olfactory bulb minutes following IN administration (Fig. 3) [61]. Interestingly, although OEC express the TJ proteins ZO-1, occludin, and claudin-5, they maintain continuous open spaces for the regrowth of olfactory nerve fibers, creating an additional extracellular path that substances may take to reach the brain along with entering olfactory nerve bundles [49,62]. Finally, the perineural spaces of cranial nerves such as the olfactory and trigeminal nerves appear to allow communication with the CSF of the subarachnoid space for some substances, providing a potential route for molecules to reach the CNS from the nasal cavity [59]. Substances accessing the subarachnoid space CSF following IN administration could potentially distribute along pathways of CSF flow to other, more distant sites. Interestingly, not all proteins transported to the CNS following IN administration are detectable within the CSF (e.g. [^{125}I]-insulin-like growth factor-1 (IGF-1) is not present in cisternal CSF samples despite significant brain delivery in the rat following IN administration [36]), suggesting that substances do not have to enter the CSF in order to access the brain.

We have previously shown that [^{125}I]-labeled proteins such as insulin-like growth factor-1 (IGF-1) and interferon-β1b (INF-β1b) rapidly distribute along pathways associated with the trigeminal and olfactory nerves to reach both rostral and caudal brain regions in rats and cynomolgus monkeys within 30–60 min after beginning IN application (Fig. 4) [36,37]. What may we conclude about the most likely mechanism underlying transport from the nasal mucosa to brain entry sites from the distribution and kinetics of entry for these proteins? The average distance from the olfactory epithelium to the olfactory bulb (olfactory pathway; Fig. 5A) in an adult rat can be estimated (~4–5 mm) from periodic acid-Schiff stained whole mounts of the nasal passage, in which the olfactory region is

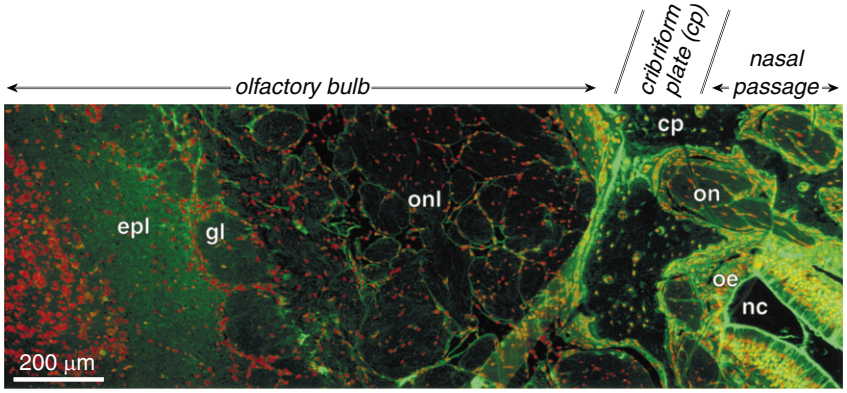

Fig. 3. Distribution of fluorescein-labeled 3 kDa dextran (green) in the olfactory epithelium (oe), cribriform plate (cp) area and olfactory bulb areas (olfactory nerve layer, onl; glomerular layer, gl; external plexiform layer, epl) 2 min following intranasal application in an anesthetized adult rat (nc, nasal cavity; adapted from Jansson and Bjork [61] with permission). Prominent fluorescence is observed within the perineural spaces of olfactory nerve (on) bundles in the epithelium and the onl of the olfactory bulb.

delineated by Bowman's glands [30,63]; similarly, the distance from the center of the rat nasal epithelium to the caudal brainstem (trigeminal pathway; Fig. 5A) in an adult rat can also be estimated (~20–30 mm). Assuming best case distances of 4 and 20 mm for the olfactory and trigeminal pathways respectively, it is possible to roughly calculate the expected time required for the three most obvious mechanistic possibilities that might account for experimentally observed [^{125}I]-IGF-1 delivery to the rat CNS ~30 min following IN administration [36]: intracellular (axonal) transport, extracellular diffusion, or extracellular convection (bulk flow). First, we can predict the expected time required for intracellular (axonal) transport within olfactory or trigeminal nerves to result in delivery of [^{125}I]-IGF-1 from

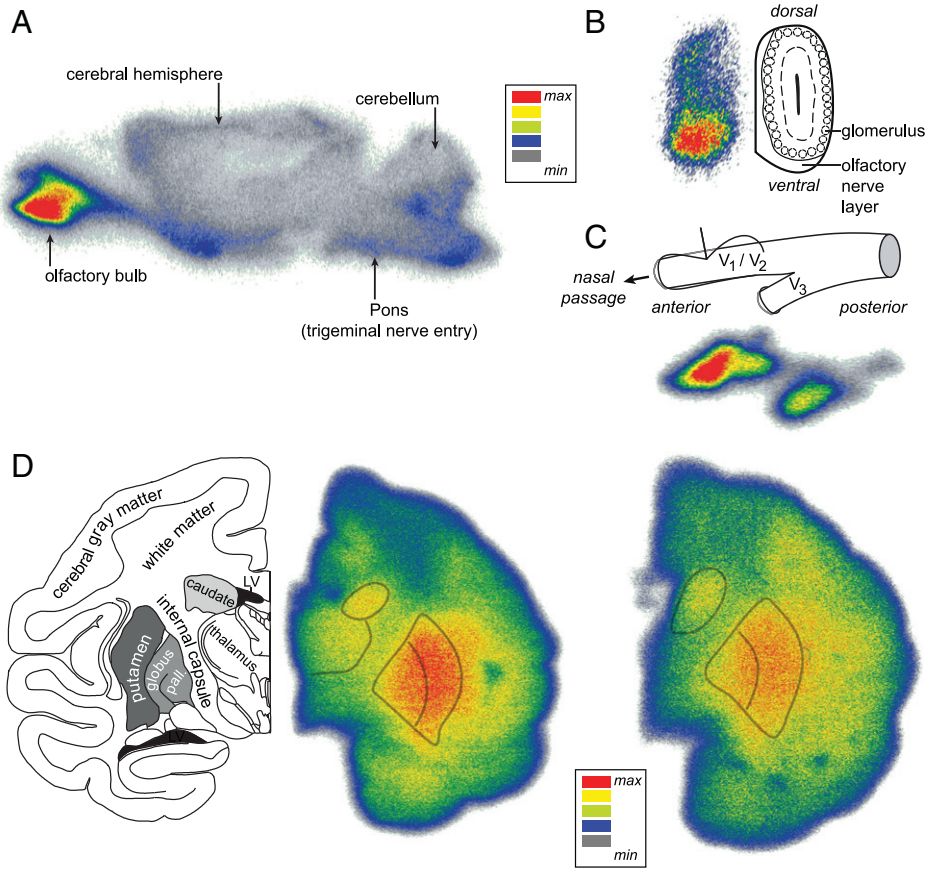

Fig. 4. Autoradiographic distribution of [^{125}I]-labeled proteins in the brain following intranasal application in anesthetized adult rats or cynomolgus monkeys. (A) Sagittal brain section from a rat approximately 30 min following intranasal administration of a low specific activity solution of [^{125}I]-labeled insulin-like growth factor-1 (7.65 kDa), allowing brain entry sites in the olfactory bulb (putative olfactory pathway) and pons (putative trigeminal pathway) to be visualized. (B) Coronal section through the olfactory bulb of a rat approximately 30 min following intranasal administration of a high specific activity solution of [^{125}I]-labeled insulin-like growth factor-1, showing strongest signal in the ventral portion of the bulb. (C) Transverse section through the trigeminal nerve of a rat approximately 30 min following intranasal administration of a high specific activity solution of [^{125}I]-labeled insulin-like growth factor-1, showing strongest signal in portions of the ophthalmic (V_1) and maxillary (V_2) nerve divisions which innervate the nasal passage. (A, B and C adapted from Thorne et al. [36] with permission.) (D) Coronal brain sections from two different monkeys approximately 60 min following intranasal administration of [^{125}I]-labeled interferon-β1b (18.5 kDa), showing strongest signal in basal ganglia components (putamen, globus pallidus and caudate). (D adapted from Thorne et al. [37] with permission).

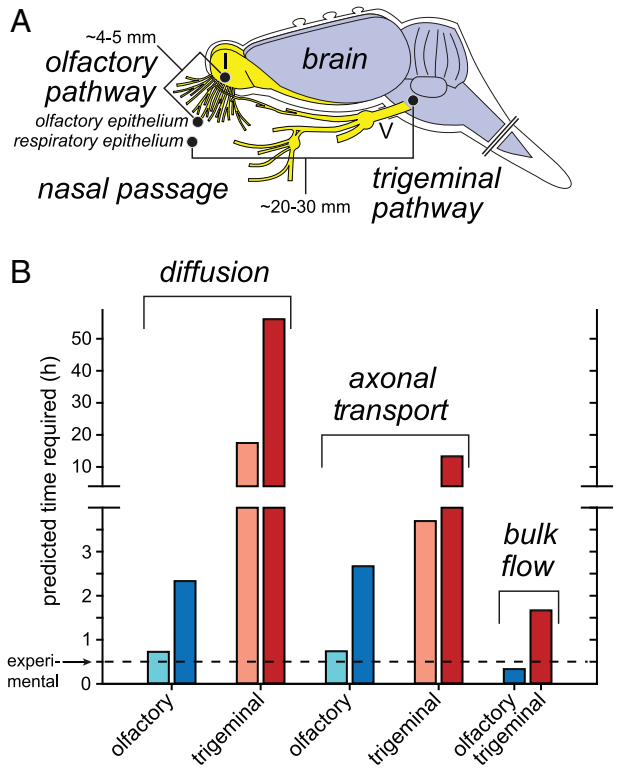

Fig. 5. Model predictions of the time required for different transport mechanisms possible for the delivery of [^{125}I]-labeled insulin-like growth factor-1 to the olfactory bulb or brainstem following intranasal administration suggests only a convective process (bulk flow) approaches being rapid enough to account for experimentally observed data. (A) Schematic showing the pathways and approximate average distances from the olfactory and respiratory epithelium to CNS targets. (B) Predicted times required for extracellular diffusion along peripheral olfactory or trigeminal components (light blue and light red bars, fast diffusion based on free diffusion coefficient in water; dark blue and dark red bars, slow diffusion based on effective diffusion coefficient in brain), intracellular (axonal) transport within olfactory or trigeminal nerves (light blue and light red bars, fast axonal transport based on protein transport rate in olfactory nerves; dark blue and dark red bars, slow axonal transport based on protein transport rate in olfactory nerves), and extracellular convection (bulk flow) along peripheral olfactory or trigeminal components. See text for additional details.

the nasal passages to the olfactory bulb or brainstem. Using published values for fast (130 mm/day) and slow (36 mm/day) axonal transport of exogenous proteins in pike olfactory nerves (corrected to 37 °C) [64], we expect it would take 0.74 h (fast)–2.7 h (slow) for intracellular transport within olfactory neurons to the olfactory bulb and 3.7 h (fast)–13 h (slow) for intracellular transport within trigeminal ganglion cells to the brainstem, assuming similar transport rates in OSN and trigeminal ganglion cells (Fig. 5B). This estimate is in rough agreement with published data on the intracellular transport of WGA-HRP from the olfactory epithelium to the olfactory bulb, a process that takes at least 6 h in mice [40], as well as from the nasal epithelium to the trigeminal brainstem nuclear complex, a process taking as much as 48 h in rats [43]. Second, we can predict the expected time required for extracellular diffusion along components of the peripheral olfactory or trigeminal systems to result in delivery of [^{125}I]-IGF-1 from the nasal passages to the olfactory bulb or brainstem. Assuming 1-D diffusion along each pathway (with nasal epithelial concentration held constant), the following equation may be used [65]:

$$c/c_o = erfc\left(\frac{x}{2\sqrt{Dt}}\right)$$

where c = olfactory bulb or brainstem concentration of [^{125}I]-IGF-1 and c_0 = nasal epithelium concentration of [^{125}I]-IGF-1 (values obtained from Thorne et al. [36]), *erfc* is the complimentary error function, x is the pathway distance (olfactory, 4 mm; trigeminal, 20 mm), D is the diffusion coefficient for [^{125}I]-IGF-1, and t is the predicted time. If we estimate D using published free (18×10^{-7} cm^2/s) and effective (brain) diffusion coefficients (6×10^{-7} cm^2/s) for a protein, epidermal growth factor (MW = 6.6 kDa) [66], similar in size to [^{125}I]-IGF-1 (MW = 7.65 kDa), we expect it would take 0.73–2.3 h for diffusion to the olfactory bulb along olfactory-associated extracellular pathways and 17–56 h for diffusion to the brainstem along trigeminal-associated extracellular pathways (Fig. 5B). Finally, we can predict the expected time required for an extracellular convective process such as bulk flow of fluid within perivascular spaces of blood vessels traveling with the peripheral olfactory or trigeminal systems to result in delivery of [^{125}I]-IGF-1 from the nasal passages to the olfactory bulb or brainstem. Using a conservative estimate of the bulk flow rate of fluorescently labeled albumin transport within the perivascular space of cerebral arteries on the pial surface of the rat brain (~200 μm/min) [67], we expect it might take at most 0.33 h for extracellular bulk flow to the olfactory bulb within perivascular spaces associated with the peripheral olfactory system and 1.7 h for extracellular bulk flow to the brainstem within perivascular spaces associated with the peripheral trigeminal system (Fig. 5B). It is likely that the bulk flow transport rate within the cerebral perivascular spaces may be considerably higher than estimates from open cranial window preparations where normal intracranial pressure is altered to allow for fluorescence imaging (such as in ref. 67); significantly higher bulk flow rates within the perivascular spaces or other olfactory/trigeminal components could allow for substantially shorter times required for delivery, as demonstrated in some studies. While other possibilities may exist, the above calculations strongly suggest the only plausible transport process that could account for the experimental results following IN administration of [^{125}I]-IGF-1 is convection (bulk flow) along olfactory and trigeminal nerve components to brain entry sites.

3.3. Transport from brain entry sites to other CNS areas

Final distribution from drug entry points at the level of the olfactory bulb and brainstem to other areas of the CNS may be envisioned to occur either by *intracellular* transport (i.e. transfer and uptake to second order neurons synapsing with peripheral OSN or trigeminal ganglion cells) or *extracellular* transport (e.g. widespread distribution via convective transport within the cerebral perivascular spaces, local diffusion at the entry points and local diffusion from perivascular spaces into the parenchyma). As discussed above in Section 3.2, the central distribution and kinetics of brain entry measured for [^{125}I]-labeled proteins such as IGF-1 and INF-β1b suggest that rapid, extracellular flow occurs along olfactory and trigeminal nerve components in the nasal epithelium to the olfactory bulb and brainstem; the most likely convective mechanism that could explain the further distribution of these proteins from olfactory and trigeminal brain entry points to other, distant CNS sites is bulk flow within the perivascular spaces of cerebral blood vessels. It has been speculated that expansion and contraction of the perivascular spaces with the cardiac cycle could generate a pronounced fluid flow within them under normal conditions; different groups have attempted to understand the direction and characteristics of this flow by modeling the process but have produced different results [68,69]. Another group of investigators have shown that increasing the blood pressure and heart rate results in a larger distribution of adeno-associated virus 2 capsids or fluorescent liposomes after injection into the striatum, suggesting involvement of arterial pulsations in the intraparenchymal distribution of these large substances via the perivascular spaces [70]. Other possibilities of course exist. One group has recently suggested that the rostral

migratory stream, the pathway used by neuronal progenitors to migrate from periventricular regions to the olfactory bulb, may also play a role in the delivery of molecules from the nasal cavity to the brain [71]. They observed that surgical transection of the rostral migratory stream significantly reduced the levels of [^{125}I]-calcitonin and [^{125}I]-erythropoietin (EPO) in the brain following IN administration.

4. Intranasal delivery of biologics to the central nervous system

4.1. Animal data

Numerous studies have demonstrated IN drug delivery to effectively treat animal models of CNS diseases. Most of these studies did not show pharmacokinetic data which clearly demonstrated brain uptake of the nasally administered compound but rather presented pharmacodynamic data showing a positive effect following IN delivery of a substance in an animal model. This makes it difficult to ascertain whether the drug bypassed the BBB via direct nose-to-brain pathways to enter the CNS, crossed the BBB to enter the CNS or perhaps exerted its effects by acting on the brain endothelium. Our review will emphasize those studies utilizing IN delivery of biologics which have pharmacokinetic data to support their ability to directly enter the CNS from the nasal cavity.

4.1.1. Peptides

Insulin (MW = 5.8 kDa) is a peptide which has effects well known in regulating energy metabolism, but it also has a signaling role in the CNS due to expression of the insulin receptor in the brain [72]. [^{125}I]-insulin distributes widely throughout the mouse brain 1 h following IN administration, with the highest levels detected in the trigeminal nerve and the olfactory bulbs [73]. Levels of [^{125}I]-insulin in the CNS were significantly higher than levels measured following subcutaneous injection of [^{125}I]-insulin at this time point. IN insulin also slowed development of cognitive decline, ameliorated magnetic resonance imaging abnormalities, prevented morphological abnormalities in the cerebrum, and improved mortality in a mouse model of type I diabetes [73]. Changes in mRNA and/or protein levels of phosphoinositide 3-kinase/Akt, cyclic AMP response element binding protein, glycogen synthase kinase 3β, synaptophysin, and choline acetyltransferase (ChAT) were also prevented by IN insulin in the same mice. IN [^{125}I]-insulin has also been found to yield higher levels in the spinal cord than subcutaneous [^{125}I]-insulin 1 h post-delivery [74]. IN insulin improved neuropathic pain, electrophysiological and morphological abnormalities, and prevented changes in the expression of phosphoinositide 3-kinase/Akt, cyclic AMP response element binding protein, and glycogen synthase kinase-3β within dorsal root ganglia in a mouse model of diabetic neuropathy [74]. Increases in short- and long-term object memory recognition, anxiolytic behavior, and odor discrimination have also been observed in mice following IN insulin administration [75]. These changes were attributed to suppression of a dominant Shaker ion channel (Kv1.3).

The peptide [Ser(2)]exendin(1–9) (MW = 980 Da) is homologous to a conserved domain in the glucagon/glucagon-like peptide-1 family, allowing it to act as an agonist at the GLP-1 receptor (GLP-1R). IN [Ser(2)]exendin has been found to facilitate learning and lead to lower rates of kainic acid-induced apoptosis in mice, effects that were likely mediated through expression of the GLP-1R in the hippocampus [76]. Brain distribution of the GLP-1 antagonist exendin(9–39) (Ex) (MW = 3.4 kDa) has also been compared after IN and IV administration by Banks et al. [77]. IN [^{131}I]-Ex resulted in a higher brain/serum ratio compared to IV administration 10 min after dosing and was found to distribute to the olfactory bulb, anterior brain, hippocampus, cerebellum, and brain stem. [^{131}I]-Ex was detected in the CSF at levels intermediate between the olfactory bulb and the whole brain. This study also attempted to examine the mechanism of [^{131}I]-Ex distribution by intranasally applying [^{131}I]-Ex to mice that had been dead for about 10 min. The amount of [^{131}I]-Ex found in the brain and olfactory bulbs of dead mice was markedly lower than live mice. This suggested to the authors that IN [^{131}I]-Ex was transported by a bulk flow mechanism (energy dependent) rather than diffusion, although reduction of the brain extracellular space following terminal ischemia would also have likely altered diffusion, complicating interpretation of the data [78].

Galanin-like peptide (GALP) (MW = 6.5 kDa) is a neuropeptide that holds promise in treating obesity [79]. IN [^{131}I]-GALP has resulted in delivery to the olfactory bulb, anterior brain, hippocampus, hypothalamus, cerebellum, brain stem, and CSF in mice [80]. Relative to IV injection, IN delivery of [^{131}I]-GALP produced 20-fold greater levels in the CNS. This effect was increased 2–3-fold when the absorption enhancer α-cyclodextrin was co-administered.

Orexin-A (MW = 3.6 kDa) is a sleep-related peptide produced in the hypothalamus. When administered to sleep-deprived rhesus monkeys, orexin-A improved task performance and induced changes in brain metabolic activity [81]. These effects were more pronounced in monkeys given orexin-A intranasally compared to monkeys administered an IV dose. Orexin-A distributed to the brain within 30 min in rats after nasal administration and tissue-to-blood concentration ratios were 5–8 times higher in the posterior trigeminal nerve, olfactory bulbs, hypothalamus, and cerebellum compared to rats given orexin-A IV [82]. High levels of orexin-A were found in cerebral blood vessel walls while very little was found in the CSF of these rats, suggesting the transport pathways may have involved distribution within the perivascular spaces.

NAP is an eight amino acid peptide (MW = 825 Da) derived from activity dependent neurotrophic factor. IN administration produced intact levels of [^{3}H]-labeled NAP in the cortex and cerebellum of rats within 30 min [83]. NAP delivered intranasally improved memory in normal and cognitively impaired rats and decreased anxiety-like behavior in aged mice [83,84]. In a mouse model of Alzheimer's disease, IN NAP significantly reduced levels of beta-amyloid (Aβ) and hyperphosphorylated tau [85]. Chronic IN administration of NAP increased spatial learning and memory, increased soluble tau, and decreased neurofibrillary tangles in a mouse model of tauopathy [86]. In stable tubule-only polypeptide heterozygous mice, a mouse model of schizophrenia, NAP decreased hyperactivity and protected visual memory [87]. Further, oxidative stress was reduced and memory function was improved by IN administration of NAP in rats subjected to chronic hypoxia [88].

IN delivery of calcitonin gene-related peptide (MW = 3.8 kDa) has been shown to significantly reduce vasospasm, improve cerebral blood flow, reduce cortical and endothelial cell death, increase the levels of vascular endothelial growth factor (VEGF) and stimulate angiogenesis in a rat model of subarachnoid hemorrhage [89]. The same study also showed IN administration of radiolabeled calcitonin gene-related peptide resulted in significantly higher levels in the CSF, cortex, and hippocampus relative to IV administration.

The neuropeptide pituitary adenylate cyclase-activating polypeptide (PACAP) (MW = 4.5 kDa) has been shown to produce beneficial effects in an AD model following chronic IN administration [90]. IN [^{125}I]-PACAP reached the brain after 5 min and was detected intact 30 min after application. PACAP improved cognitive function and stimulated non-amyloidogenic processing of the amyloid precursor protein. Levels of brain-derived neurotrophic factor as well as the anti-apoptotic protein Bcl-2 were increased. In addition, expression of the Aβ-degrading enzyme neprilysin was induced by PACAP [90].

4.1.2. Proteins

One of the best characterized proteins delivered to the brain by the intranasal route has been IGF-1 (MW = 7.65 kDa). IN [^{125}I]-IGF-1 has been shown to yield significantly higher CNS concentrations than comparable IV dosing with [^{125}I]-IGF-1; studies with IGF-1 were

also the first to implicate widespread distribution within the CNS by both olfactory and trigeminal nerve pathways [36]. IN administration of IGF-1 resulted in phosphorylation of extracellular signal-regulated kinase 2 and p130 Crk-associated substrate in the brain [36]. In a middle cerebral artery occlusion (MCAO) stroke model, IN IGF-1 administered 10 min, 24 h, and 48 h after 2 h MCAO significantly reduced infarct volume and brain edema and significantly improved neurologic function [91,92]. Even when first given 2 h after MCAO, IN IGF-1 significantly reduced infarct volume, improved neurologic deficit scores, and inhibited apoptosis [93]. IN administration of recombinant human IGF-1 also enhanced neurobehavioral performance, inhibited apoptotic cell death, and enhanced proliferation of neuronal and oligodendroglial progenitors when administered 1 h after hypoxic–ischemic brain injury in neonatal rats [94].

Erythropoietin (EPO) (MW = 30–34 kDa) is a hematopoietic growth factor that shows neuroprotection in various models of brain injury, including stroke [95]. To test if intranasal administration of recombinant human EPO (rhEPO) was neuroprotective in a model of transient cerebral ischemia (1 h MCAO followed by reperfusion), IN doses of 1.2, 4.8, 12, and 24 U or intraperitoneal doses of 5000 U/kg were administered to rats 10 min after MCAO and 1 h following reperfusion [96]. It was found that IN doses of 4.8 and 12 U rhEPO significantly reduced the infarct volume and the neurological score similar to intraperitoneal 5000 U/kg. Furthermore, heat-inactivated rhEPO administered intranasally had no effect. Another study found that both [^{125}I]-EPO and [^{125}I]-IGF-1 were detected in the brain 20 min after IN administration [97]. When compared to IV, intraperitoneal, and subcutaneous injections, IN administration resulted in significantly higher levels of both compounds in normal brains as well as in the brains of mice which underwent MCAO. The IN combination of EPO and IGF-1 delivered 1 h after MCAO significantly reduced infarct volumes 24 h later and improved neurological function up to 90 days later. A combination of IN EPO and IGF-1 was also shown to be neuroprotective in gp120 transgenic mice, a model of human immunodeficiency virus infection [98]. Finally, another study showed that IN administration of radiolabeled EPO, brain derived neurotrophic factor (MW = 27 kDa), ciliary neurotrophic factor (MW = 22.7 kDa), or neurotrophin-4 (MW = 22.4 kDa) also resulted in widespread CNS delivery with highest levels observed in the trigeminal nerve 25 min after administration [99] .

IFN-β1b (MW = 18.5 kDa) is an anti-inflammatory cytokine used to treat multiple sclerosis. IV [^{125}I]-IFN-β1b has been shown to yield significantly lower CNS levels than IN [^{125}I]-IFN-β1b using doses that resulted in similar blood concentrations in rats [100]. High levels of IN [^{125}I]-IFN-β1b were detected in the olfactory bulbs, trigeminal nerve and deep cervical lymph nodes with lower levels in other brain regions and the spinal cord. Importantly, [^{125}I]-IFN-β1b was shown to reach the brain intact while separate experiments also demonstrated IN IFN-β1b produced tyrosine phosphorylation of the IFN receptor. Widespread CNS distribution of [^{125}I]-IFN-β1b was shown in a later study following IN administration in cynomolgus monkeys [37]; this study implicated olfactory and trigeminal pathways into the primate CNS, as previously demonstrated in the rat, and also demonstrated a unique anatomical concentration of [^{125}I]-IFN-β1b within components of the basal ganglia. Although primates have a much smaller nasal epithelium relative to brain size than rodents, this study was notable for showing that large MW therapeutics administered intranasally to primates are also capable of reaching the CNS, with bioactive levels possible in many interior (deep) brain regions.

Ovalbumin (MW = 45 kDa) has been demonstrated in the substantia nigra and striatum 6 h and 24 h after IN administration [101]. Higher levels were detected when ovalbumin was delivered in cationic liposomes. Due to the involvement of the substantia nigra and striatum in the pathogenesis of Parkinson's disease, the IN route may hold great promise for the delivery of biologics to treat Parkinson's disease.

Several studies have looked at intranasal administration of the obesity-related protein leptin (MW = 16 kDa). Although the BBB has the ability to transport leptin into the CNS from the blood, this transport is impaired during obesity [102], making intranasal delivery of leptin into the CNS a potential strategy to regulate feeding behavior (Table 4). A pharmacokinetic study of IN [^{125}I]-leptin showed that 81.5% was delivered intact to the CNS within 30 min, with highest levels in the hypothalamus [103]. Excess leptin given IV did not diminish brain uptake of [^{125}I]-leptin, consistent with a direct nose-to-brain pathway rather than specific uptake across the BBB. Very little [^{125}I]-leptin was recovered in the CSF, suggesting that brain distribution did not result from CSF circulation. A study looking at leptin's effects on feeding behavior found male rats given leptin intranasally for 4 weeks gained significantly less weight and consumed significantly less food and water than control rats [104]. These same rats showed a significant increase of corticotropin-releasing factor mRNA in the central nucleus of the amygdala while serum levels of leptin remained unchanged. Another study concluded that intranasal leptin caused longer inhibition of appetite and an increase in phosphorylated signal transducer and activator of transcription 3 in the arcuate nucleus of the hypothalamus when compared to intraperitoneal injection of leptin [105]. Intranasal administration of leptin has also been shown to delay the onset of pentylenetetrazole-induced generalized convulsive seizures in mice [106].

Recombinant human nerve growth factor (NGF) (MW = 26.5 kDa) has been shown to reach the olfactory bulb, cortex, cerebellum, brain stem, hippocampus, and amygdala in significantly higher concentrations 30–45 min following IN administration as compared with a matched IV dose [107]. Further, IN delivery of NGF in a NGF-deficient transgenic mouse model of AD has been shown to result in increased basal forebrain ChAT expression, decreased Aβ accumulation, and rescue of recognition memory deficits [108,109]. Antidepressant-like effects in rats have also been observed following IN NGF administration [110]. Finally, IN NGF has enhanced neurogenesis in the striatum and improved functional recovery when administered 24 h following MCAO [111].

Direct transport of VEGF (MW = 38.2 kDa) to the CNS has also been shown following intranasal administration [112]. [^{125}I]-VEGF was delivered to the brain 30 min after IN administration and was detected as a higher percentage of the initial dose in the olfactory bulb, olfactory tubercle, striatum, thalamus, hippocampus, midbrain, pons, cerebellum, medulla, and frontal cortex when administered intranasally compared to intravenously. [^{125}I]-VEGF was not found in the CSF following intranasal administration [112]. Intranasal delivery of recombinant human VEGF also reduced infarct volume, improved behavioral recovery, and enhanced angiogenesis following MCAO in rats [113].

Recombinant human transforming growth factor β1 (TGF-β1) (MW = 25 kDa) was found significantly increased in the olfactory bulb, striatum, thalamus, cortex, and trigeminal nerve within 30 min following IN administration when compared to vehicle solution [114]. No increase in TGF-β1 was observed in the plasma or peripheral organs, suggesting direct nose-to-brain uptake. TGF-β1 remained significantly increased in the olfactory tubercle, striatum, thalamus, hippocampus, and cortex 6 h after IN administration and was not detected in the CSF at any time point [114]. Following MCAO in mice, IN delivery of TGF-β1 reduced infarct volume, improved functional recovery, and increased neurogenesis in the subventricular zone [115].

Levels of recombinant human basic fibroblast growth factor (MW = 17.2 kDa) were significantly increased in the olfactory bulb and the striatum of rats following IN administration [116]. When basic fibroblast growth factor was delivered intranasally following cerebral ischemia/reperfusion, improved neurological function and reduced infarct volume were observed [116]. Rats which received IN

Table 4
Summary of intranasal delivery of peptides/proteins to CNS.

	Molecular weight	Pharmacokinetic data	Pharmacodynamic data
Preclinical biologic			
NAP [83–85,87,88]	825 Da	Detected in brain, CSF levels not determined	Improved memory; reduced AD-like pathology; decreased hyperactivity; reduced hypoxia-induced oxidative stress
[Ser(2)]exendin(1–9) [76]	980 Da	Not determined	Facilitated learning; reduced kainic-acid induced apoptosis
Exendin(9–39) [77]	3.4 kDa	Detected in brain and CSF	Not determined
Orexin-A (hypocretin-1) [81,82]	3.6 kDa	Detected in brain, small amount in CSF	Improved task performance following sleep deprivation
Calcitonin gene-related peptide [89]	3.8 kDa	Detected in brain and CSF	Reduced vasospasm, improved cerebral blood flow, reduced cell death, and stimulated angiogenesis following subarachnoid hemorrhage
Pituitary adenylate cyclase-activating peptide [90]	4.5 kDa	Detected in brain, CSF levels not determined	Stimulated non-amyloidogenic processing and improved cognitive function in an AD model
Insulin [72–75]	5.8 kDa	Detected in brain, CSF levels not determined	Slowed cognitive decline, improved mortality, and reduced neuropathic pain in a model of type I diabetes; improved memory recognition, anxiolytic behavior, and odor discrimination
Galanin-like peptide [79]	6.5 kDa	Detected in brain and CSF	Not determined
Insulin-like growth factor 1 [36,89–92]	7.65 kDa	Detected in brain, no CSF detection	Reduced infarct volume/brain edema, and improved neurologic function in stroke models; inhibited apoptosis following hypoxic–ischemic injury in neonatal rats
Leptin [102–106]	16 kDa	Detected in brain, small amount in CSF	Inhibited appetite; decreased weight gain
Recombinant human basic fibroblast growth factor [116,117]	17.2 Da	Detected in brain, CSF levels not determined	Improved neurological function, reduced infarct volume and enhanced neurogenesis in stroke models
Interferon β1b [37,100]	18.5 kDa	Detected in brain, CSF levels not determined	Phosphorylated INF receptor
Neurotrophin-4 [99]	22.4 kDa	Detected in brain, CSF levels not determined	Not determined
Ciliary neurotrophic factor [99]	22.7 kDa	Detected in brain, CSF levels not determined	pAkt activated in occipital cortex
Transforming growth factor β1 [114,115]	25 kDa	Detected in brain, no CSF detection	Reduced infarct volume, improved functional recovery, and increased neurogenesis in stroke models
Single-chain antibody fragment [119,120]	26.3 kDa	Detected in brain, CSF levels not determined	Reduced cerebral amyloid angiopathy and amyloid plaque pathology in AD models
Nerve growth factor [107–111]	26.5 kDa	Detected in brain, CSF levels not determined	Decreased Aβ accumulation, and improved memory in AD models; antidepressant-like effects/enhanced neurogenesis and improved functional recovery in stroke models
Brain derived neurotrophic factor [99]	27 kDa	Detected in brain, CSF levels not determined	pAkt activated in frontal cortex
Erythropoietin [96,97]	30–34 kDa	Detected in brain, CSF levels not determined	Reduced infarct volume and improved neurologic function in stroke models
Vascular endothelial growth factor [112,113]	38.2 kDa	Detected in brain, no CSF detection	Reduced infarct volume, improved behavioral recovery, and enhanced neurogenesis in stroke models
Ovalbumin [101]	45 kDa	Detected in brain, CSF levels not determined	Not determined
Full length IgG [121,122]	150 kDa	Not determined	Anti-amnesic effect in an AD model; improved conditioned passive avoidance response following ischemia
Clinical biologic			
Melanocortin(4–10)(MSH/ACTH(4–10)) [137–140]	980 Da	Detected in CSF	Acutely diminished focusing of attention; decreased body fat in normal weight humans
Angiotensin II (ANG II) [135]	1.0 kDa	Not determined	Acutely increased blood pressure; maintained plasma norepinephrine levels
Arginine-vasopressin (AVP) [133]	1.1 kDa	Detected in CSF	Increased brain activity
Cholecystokinin-8 [134]	1.1 kDa	Not determined	Increased brain activity
Oxytocin [148–153]	1 kDa	Not determined	Increased trust; reduced stress-related cortisol; improved ability to infer mental state of others; produced anxiolytic effects; attenuated response to fear in amygdala in generalized anxiety disorder; improved emotional recognition in autism
Insulin [141–145]	5.8 kDa	Detected in CSF	Reduced brain activity; decreased food intake; enhanced postprandial thermogenesis; improved memory and modulated Aβ in patients with MCI

basic fibroblast growth factor daily for 6 days starting one day after MCAO also showed enhanced neurogenesis [117].

Antibodies are very useful therapeutics due to their ability to bind and neutralize peptides and proteins in a highly specific manner; however, they only show limited penetration into the brain when delivered peripherally [118]. Only a few studies have been conducted looking at IN administration of an antibody to the CNS. ESBA105A is a single-chain F_v antibody fragment (MW = 26.3 kDa) which binds to and inhibits tumor necrosis factor α. A study looking at distribution of ESBA105A found higher levels in the olfactory bulb, cerebrum, cerebellum, and the brainstem with similar levels in the serum 4 h after IN delivery as compared to IV administration [119]. An anti-$A\beta_{30-42}$ single chain F_v antibody fragment was administered intranasally twice a week for 14 weeks in a transgenic mouse model of AD [120]. This treatment resulted in a reduction of cerebral amyloid angiopathy and plaque pathology. Additionally, the single chain F_v antibody was detected bound to amyloid plaques in the brains of these mice. IN delivery of full-length antibodies to glutamate (MW = 150 kDa) has resulted in anti-amnesic effects in rats subjected to prior injection with an Aβ fragment ($A\beta_{25-35}$) into the nucleus basalis of Meynert; IN administration of the same antibody also improved retention of the conditioned passive avoidance

response in rats with ischemic injury of the prefrontal cortex, although neither study examined antibody pharmacokinetics within the brain [121,122].

4.1.3. Gene vectors

Delivery of gene vectors to the CNS represents an attractive strategy to induce or repress long term expression of a peptide or protein of therapeutic interest. It is difficult to surpass the BBB with gene vectors, however, making IN administration a potentially attractive alternative route.

The recombinant adenoviral vector ADRSVβgal has been detected in the brain of rats after IN administration [123]. β-galactosidase activity was detected in the olfactory bulb, locus ceruleus, area postrema, brainstem, and hippocampus 12 days following IN delivery.

IN administration has been shown to effectively deliver plasmid DNA to the brain [124]. The 7.2 kb pCMVβ and the 14.2 kb pN2/CMVβ which encoded the β-galactosidase gene were detected in the brain within 15 min of IN administration [125]. β-galactosidase activity was significantly higher in brain homogenates 48 h later. The brain-to-serum ratio of pCMVβ levels was ~2600 times higher 10 min after IN administration when compared to IV administration, with pCMVβ detected at higher levels in the olfactory bulb, medial olfactory area, striatum, hypothalamus, thalamus, midbrain, hippocampus, medulla, and cerebellum after IN application.

The growth compromised herpes simplex virus type 2 mutant ΔRR encoding the anti-apoptotic gene ICP10PK has also been successfully delivered to the brain through the IN route [126]. ICP10PK-LacZ was detected in the amygdala, entorhinal cortex, hypothalamus, thalamus, and hippocampus. ΔRR prevented kainic acid-induced seizures, neuronal loss, and inflammation in both mice and rats.

A filamentous bacteriophage (1000 nm long, 6 nm wide) encoding the myelin oligodendrocyte protein epitope (MOG_{36-44}) fused to the main coat protein has also been delivered intranasally to treat murine experimental autoimmune encephalomyelitis [127], an animal model of multiple sclerosis. IN delivery of the phage MOG resulted in improved neuronal function and reduced levels of proinflammatory cytokines such as monocyte chemoattractant protein 1, interferon γ, and interleukin-6. There was also a depletion of autoantibodies to MOG and prevention of demyelination, resulting in improved clinical scores and reduced inflammation. A previous study detected filamentous phage, but not spheroid phage, in the brain following IN administration, suggesting that the size and/or shape of the phage may be important for its ability to enter the CNS [128].

Finally, successful delivery of small interfering RNA (siRNA) to the CNS has been demonstrated following IN delivery. FITC-labeled transfection control siRNA was detected in the olfactory bulb 12 h after IN administration [129]. IN delivery of siRNA to αB-crystallin resulted in reduced expression of αB-crystallin in neurons in astrocytes in the olfactory bulb, amygdala, entorhinal cortex, and hypothalamus 3 and 12 h following administration [129].

4.1.4. Stem cells

Stem cells are an attractive treatment option for many diseases of the CNS due to their potential ability to replace dead cells or deliver neurotrophic factors to damaged cells. Interestingly, fluorescently labeled rat mesenchymal stem cells (MSC) have been detected in the olfactory bulb, hippocampus, thalamus, cortex, and subarachnoid space of mice 1 h after IN delivery [130]. MSC have also been administered intranasally to an animal model of PD (6-hydroxydopamine-lesioned rats) [131]. MSC were detected in the olfactory bulb, cortex, hippocampus, striatum, cerebellum, brainstem, and spinal cord and 24% of these cells survived at least 4.5 months. In the striatum and substantia nigra ipsilateral to the lesion, intranasal MSC increased tyrosine hydroxylase levels, eliminated terminal deoxynucleotidyl transferase dUTP nick end labeling staining, and prevented a decrease in dopamine levels. Behavioral analyses showed significant improvement in forepaw motor function 40–110 days after IN delivery of 1×10^6 cells. IN MSC have also been used to treat ischemic brain damage in neonatal mice [132]. MSC administered intranasally 10 days following the induction of hypoxia–ischemia resulted in improved sensorimotor function and decreased brain lesion size 18 days following MSC application.

4.2. Clinical data

Importantly, a number of examples clearly show CNS effects following intranasal delivery of biologics to humans. One of the earliest studies compared IN to IV administration of arginine-vasopressin (AVP) (MW = 1.1 kDa). Plasma concentrations of vasopressin were significantly higher following IV administration of AVP but only IN administration of AVP resulted in a significant increase in the P3 component of event related potentials which measure brain activity [133]. The same group has also administered cholecystokinin-8 (MW = 1.1 kDa) to humans intranasally or intravenously [134]. IN administration resulted in a significant increase in the P3 complex of auditory evoked potentials as well as plasma corticotropin levels (interpreted as a centrally mediated effect) compared to IV cholecystokinin.

Another study compared IN and IV administration of angiotensin II (ANG II) (MW = 1.0 kDa) in men [135]. It was found that each dose resulted in equivalent increases in plasma ANG II levels and an acute increase in blood pressure. However, increased blood pressure remained only in the IV administered group. The IN administered group also counteracted the plasma decrease in norepinephrine and showed increased plasma vasopressin compared to the IV administered group. These differences may be due to ANG II binding to brain angiotensin receptors involved in centrally mediated regulation of blood pressure [136].

In a pioneering study by Born and colleagues (the only study to date in which CNS pharmacokinetic data has been obtained for biologics in human beings), the peptides melanocortin(4–10) (MW = 980 Da), AVP, and insulin were each administered intranasally and detected within 30 min in the CSF of healthy humans by lumbar puncture [137]. CSF concentrations remained elevated for at least 80 min and there was no increase in plasma melanocortin(4–10), insulin, or glucose, while an increase in plasma vasopressin accompanied the increase seen in the CSF [137]. In other studies by the same investigators, melanocortin(4–10) diminished focusing of attention and decreased body fat in normal weight, but not overweight humans [138–140].

Insulin is one of the most widely studied biologics with regard to its effects on the CNS following intranasal administration. Insulin delivered intranasally has been shown to significantly reduce N1 and P3 amplitudes of event related potentials as well as improve memory and mood [141,142]. In men, IN insulin decreased food intake, enhanced postprandial thermogenesis, and decreased postprandial serum insulin [143,144]. In patients with amnesic mild cognitive impairment IN insulin modulated plasma levels of Aβ and improved memory, attention, and functional status, suggesting a possible role for IN delivery of insulin in the treatment of Alzheimer's disease [145].

Oxytocin (MW = 1 kDa) is a neuropeptide with a wide range of effects on human behavior. The BBB prevents passage of peripheral oxytocin, making IN administration a potential method for assessing oxytocin's central effects [146,147]. Intranasally administered oxytocin has been shown to increase trust, improve the ability to infer the affective mental state of others, reduce cortisol levels in response to stress, produce anxiolytic effects in response to psychosocial stress, modulate connections between the amygdala and brainstem, attenuate heightened amygdala reactivity in response to fear in generalized social anxiety disorder, and improve emotional recognition in youths

with autism spectrum disorders [148–153]. These results strongly suggest that IN delivery of oxytocin may be of clinical benefit for social disorders such as anxiety, psychological stress, and autism. For a comprehensive review of oxytocin's effects in humans, see MacDonald and MacDonald or Meyer-Lindenberg et al. [154,155].

5. Conclusions

CNS drug delivery is difficult due to limitations presented by the BBB. IN delivery of drugs is a potential strategy to overcome the obstacles imposed by the BBB and is an attractive option due to its non-invasiveness. A number of animal studies have shown biologics to directly reach the brain following IN administration. Studies in humans corroborate these findings and show that IN delivery of biologics to the CNS is not unique to rodents with much smaller brains. The majority of reports have examined IN delivery of peptides or proteins, emphasizing a need for further research to be conducted with other types of macromolecules and vectors. Although the pathways and mechanisms involved in the delivery of molecules to the CNS from the nasal passages are not yet completely understood, the IN route of administration should be considered in the future by investigators for both pre-clinical and clinical studies involving treatment of diseases affecting the CNS.

Acknowledgments

This work was supported by the University of Wisconsin—Madison School of Pharmacy and the Graduate School at the University of Wisconsin. The authors thank Daniel Wolak and Mohan Gautam (University of Wisconsin—Madison) for reviewing the manuscript. RGT acknowledges (i) periodically receiving honoraria for speaking to organizations within academia, foundations, and the biotechnology and pharmaceutical industry and (ii) occasional service as a consultant on CNS drug delivery to industry.

References

[1] T.S. Reese, M.J. Karnovsky, Fine structural localization of a blood–brain barrier to exogenous peroxidase, J. Cell Biol. 34 (1967) 207–217.
[2] C. Crone, S.P. Olesen, Electrical resistance of brain microvascular endothelium, Brain Res. 241 (1982) 49–55.
[3] A.M. Butt, H.C. Jones, N.J. Abbott, Electrical resistance across the blood–brain barrier in anaesthetized rats: a developmental study, J. Physiol. 429 (1990) 47–62.
[4] W.A. Banks, Characteristics of compounds that cross the blood–brain barrier, BMC Neurol. 9 (Suppl 1) (2009) S3.
[5] A.P. Dick, S.I. Harik, A. Klip, D.M. Walker, Identification and characterization of the glucose transporter of the blood–brain barrier by cytochalasin B binding and immunological reactivity, Proc. Natl. Acad. Sci. U.S.A. 81 (1984) 7233–7237.
[6] W.A. Jefferies, M.R. Brandon, S.V. Hunt, A.F. Williams, K.C. Gatter, D.Y. Mason, Transferrin receptor on endothelium of brain capillaries, Nature 312 (1984) 162–163.
[7] W.A. Banks, The blood–brain barrier: connecting the gut and the brain, Regul. Pept. 149 (2008) 11–14.
[8] D.S. Miller, Regulation of P-glycoprotein and other ABC drug transporters at the blood–brain barrier, Trends Pharmacol. Sci. 31 (2010) 246–254.
[9] P.T. Ronaldson, K. Babakhanian, R. Bendayan, Drug transport in the brain, in: G. You, M.E. Morris (Eds.), Drug Transporters: Molecular Characterization and Role in Drug Disposition, Wiley-Interscience, Hoboken, 2007, pp. 411–461.
[10] E. Neuwelt, N.J. Abbott, L. Abrey, W.A. Banks, B. Blakley, T. Davis, B. Engelhardt, P. Grammas, M. Nedergaard, J. Nutt, W. Pardridge, G.A. Rosenberg, Q. Smith, L.R. Drewes, Strategies to advance translational research into brain barriers, Lancet Neurol. 7 (2008) 84–96.
[11] H.R. Costantino, L. Illum, G. Brandt, P.H. Johnson, S.C. Quay, Intranasal delivery: physicochemical and therapeutic aspects, Int. J. Pharm. 337 (2007) 1–24.
[12] A.B. Lansley, G.P. Martin, Nasal drug delivery, in: A.M. Hillery, A.W. Lloyd, J. Swarbrick (Eds.), Drug Delivery and Targeting, CRC Press, Boca Raton, 2001, pp. 237–268.
[13] R.G. Thorne, C.R. Emory, T.A. Ala, W.H. Frey II, Quantitative analysis of the olfactory pathway for drug delivery to the brain, Brain Res. 692 (1995) 278–282.
[14] W.H. Frey II, J. Liu, C. X., R.G. Thorne, J.R. Fawcett, T.A. Ala, Y.E. Rahman, 87–92, Delivery of 125I-NGF to the brain via the olfactory route, Drug Deliv. 4 (1997) 87–92.
[15] S.V. Dhuria, L.R. Hanson, W.H. Frey II, Intranasal delivery to the central nervous system: mechanisms and experimental considerations, J. Pharm. Sci. 99 (2010) 1654–1673.
[16] H. Baker, M.B. Genter, The olfactory system and the nasal mucosa as portals of entry of viruses, drugs, and other exogenous agents into the brain, in: R.L. Doty (Ed.), Handbook of Olfaction and Gustation, Marcel Dekker, Inc., New York, 2003, pp. 549–573.
[17] L. Illum, Is nose-to-brain transport of drugs in man a reality? J. Pharm. Pharmacol. 56 (2004) 3–17.
[18] J.R. Harkema, S.A. Carey, J.G. Wagner, The nose revisited: a brief review of the comparative structure, function, and toxicologic pathology of the nasal epithelium, Toxicol. Pathol. 34 (2006) 252–269.
[19] J.M. DeSesso, The relevance to humans of animal models for inhalation studies of cancer in the nose and upper airways, Qual. Assur. 2 (1993) 213–231.
[20] P. Field, Y. Li, G. Raisman, Ensheathment of the olfactory nerves in the adult rat, J. Neurocytol. 32 (2003) 317–324.
[21] S.T. Carmichael, M.C. Clugnet, J.L. Price, Central olfactory connections in the macaque monkey, J. Comp. Neurol. 346 (1994) 403–434.
[22] C.C. Hegg, M. Irwin, M.T. Lucero, Calcium store-mediated signaling in sustentacular cells of the mouse olfactory epithelium, Glia 57 (2009) 634–644.
[23] N. Iwai, Z. Zhou, D.R. Roop, R.R. Behringer, Horizontal basal cells are multipotent progenitors in normal and injured adult olfactory epithelium, Stem Cells 26 (2008) 1298–1306.
[24] M. Caggiano, J.S. Kauer, D.D. Hunter, Globose basal cells are neuronal progenitors in the olfactory epithelium: a lineage analysis using a replication-incompetent retrovirus, Neuron 13 (1994) 339–352.
[25] B.P. Menco, J.E. Jackson, A banded topography in the developing rat's olfactory epithelial surface, J. Comp. Neurol. 388 (1997) 293–306.
[26] B.W. Jafek, Ultrastructure of human nasal mucosa, Laryngoscope 93 (1983) 1576–1599.
[27] L. D.C., C. D.M., Anatomy of the human nasal passages, in: D. R.L. (Ed.), Handbook of Olfaction and Gustation, Marcel Dekker, Inc, New York, 1995, pp. 53–73.
[28] M. Schuenke, E. Schulte, U. Schumacher, Head and Neuroanatomy, Thieme, Stuttgart New York, 2010.
[29] T.E. Finger, V.L. St Jeor, J.C. Kinnamon, W.L. Silver, Ultrastructure of substance P- and CGRP-immunoreactive nerve fibers in the nasal epithelium of rodents, J. Comp. Neurol. 294 (1990) 293–305.
[30] F. Bojsen-Moller, Demonstration of terminalis, olfactory, trigeminal and perivascular nerves in the rat nasal septum, J. Comp. Neurol. 159 (1975) 245–256.
[31] B. Bryant, W.L. Silver, Chemesthesis: The Common Chemical Sense, in: T.E. Finger, W.L. Silver, D. Restrepo (Eds.), The Neurobiology of Taste and Smell Wiley-Liss, New York, 2000, pp. 73–100.
[32] D. Tucker, Nonolfactory responses from the nasal cavity: Jacobsen's organ and the trigeminal system, in: L.M. Biedler (Ed.), Handbook of Sensory Physiology, Springer-Verlag, New York, 1971, pp. 151–181.
[33] M.L. Schaefer, B. Bottger, W.L. Silver, T.E. Finger, Trigeminal collaterals in the nasal epithelium and olfactory bulb: a potential route for direct modulation of olfactory information by trigeminal stimuli, J. Comp. Neurol. 444 (2002) 221–226.
[34] Gray's Anatomy, 40 ed Elsevier, Philadelphia, 2008.
[35] E.C. Greene, Anatomy of the Rat, Braintree Scientific, inc., Braintree, 1935.
[36] R.G. Thorne, G.J. Pronk, V. Padmanabhan, W.H. Frey 2nd, Delivery of insulin-like growth factor-I to the rat brain and spinal cord along olfactory and trigeminal pathways following intranasal administration, Neuroscience 127 (2004) 481–496.
[37] R.G. Thorne, L.R. Hanson, T.M. Ross, D. Tung, W.H. Frey 2nd, Delivery of interferon-beta to the monkey nervous system following intranasal administration, Neuroscience 152 (2008) 785–797.
[38] R.L. Doty, The olfactory vector hypothesis of neurodegenerative disease: is it viable? Ann. Neurol. 63 (2008) 7–15.
[39] K. Kristensson, Y. Olsson, Uptake of exogenous proteins in mouse olfactory cells, Acta Neuropathol. 19 (1971) 145–154.
[40] R.D. Broadwell, B.J. Balin, Endocytic and exocytic pathways of the neuronal secretory process and trans-synaptic transfer of wheat germ agglutinin-horseradish peroxidase in vivo, J. Comp. Neurol. 242 (1985) 632–650.
[41] H. Baker, R.F. Spencer, Transneuronal transport of peroxidase-conjugated wheat germ agglutinin (WGA-HRP) from the olfactory epithelium to the brain of the adult rat, Exp. Brain Res. 63 (1986) 461–473.
[42] K. Kristensson, Microbes' roadmap to neurons, Nat. Rev. Neurosci. 12 (2011) 345–357.
[43] F. Anton, P. Peppel, Central projections of trigeminal primary afferents innervating the nasal mucosa: a horseradish peroxidase study in the rat, Neuroscience 41 (1991) 617–628.
[44] A.M. Deatly, A.T. Haase, P.H. Fewster, E. Lewis, M.J. Ball, Human herpes virus infections and Alzheimer's disease, Neuropathol. Appl. Neurobiol. 16 (1990) 213–223.
[45] Y. Jin, L. Dons, K. Kristensson, M.E. Rottenberg, Neural route of cerebral *Listeria monocytogenes* murine infection: role of immune response mechanisms in controlling bacterial neuroinvasion, Infect. Immun. 69 (2001) 1093–1100.
[46] B.J. Balin, R.D. Broadwell, M. Salcman, M. el-Kalliny, Avenues for entry of peripherally administered protein to the central nervous system in mouse, rat, and squirrel monkey, J. Comp. Neurol. 251 (1986) 260–280.
[47] K. Hosoya, H. Kubo, H. Natsume, K. Sugibayashi, Y. Morimoto, S. Yamashita, The structural barrier of absorptive mucosae: site difference of the permeability of fluorescein isothiocyanate-labelled dextran in rabbits, Biopharm. Drug Dispos. 14 (1993) 685–695.

[48] Y. Rojanasakul, L.Y. Wang, M. Bhat, D.D. Glover, C.J. Malanga, J.K. Ma, The transport barrier of epithelia: a comparative study on membrane permeability and charge selectivity in the rabbit, Pharm. Res. 9 (1992) 1029–1034.
[49] H. Wolburg, K. Wolburg-Buchholz, H. Sam, S. Horvat, M.A. Deli, A.F. Mack, Epithelial and endothelial barriers in the olfactory region of the nasal cavity of the rat, Histochem. Cell Biol. 130 (2008) 127–140.
[50] A. Steinke, S. Meier-Stiegen, D. Drenckhahn, E. Asan, Molecular composition of tight and adherens junctions in the rat olfactory epithelium and fila, Histochem. Cell Biol. 130 (2008) 339–361.
[51] H. Altner, I. Altner-Kolnberger, Freeze-fracture and tracer experiments on the permeability of the zonulae occludentes in the olfactory mucosa of vertebrates, Cell Tissue Res. 154 (1974) 51–59.
[52] D. Kerjaschki, H. Horander, The development of mouse olfactory vesicles and their cell contacts: a freeze-etching study, J. Ultrastruct. Res. 54 (1976) 420–444.
[53] J.F. Hillyer, R.M. Albrecht, Gastrointestinal persorption and tissue distribution of differently sized colloidal gold nanoparticles, J. Pharm. Sci. 90 (2001) 1927–1936.
[54] N. Cauna, K.H. Hinderer, Fine structure of blood vessels of the human nasal respiratory mucosa, Ann. Otol. Rhinol. Laryngol. 78 (1969) 865–879.
[55] V. Lindner, H. Heinle, Binding properties of circulating Evans blue in rabbits as determined by disc electrophoresis, Atherosclerosis 43 (1982) 417–422.
[56] J.M. Yoffey, C.K. Drinker, The lymphatic pathway from the nose and pharynx: the absorption of dyes, J. Exp. Med. 68 (1938) 629–640.
[57] J.M. Yoffey, E.R. Sullivan, C.K. Drinker, The lymphatic pathway from the nose and pharynx: the absorption of certain proteins, J. Exp. Med. 68 (1938) 941–947.
[58] W.M. Faber, The nasal mucosa and the subarachnoid space, Am. J. Anat. 62 (1937) 121–148.
[59] M.W.B. Bradbury, H.F. Cserr, Drainage of cerebral interstitial fluid and of cerebrospinal fluid into lymphatics, in: M.G. Johnston (Ed.), Experimental Biology of the Lymphatic Circulation, Elsevier, Amsterdam and New York, 1985, pp. 355–391.
[60] M. Johnston, A. Zakharov, C. Papaiconomou, G. Salmasi, D. Armstrong, Evidence of connections between cerebrospinal fluid and nasal lymphatic vessels in humans, non-human primates and other mammalian species, Cerebrospinal Fluid Res 1 (2004) 2.
[61] B. Jansson, E. Bjork, Visualization of in vivo olfactory uptake and transfer using fluorescein dextran, J. Drug Target. 10 (2002) 379–386.
[62] Y. Li, P.M. Field, G. Raisman, Olfactory ensheathing cells and olfactory nerve fibroblasts maintain continuous open channels for regrowth of olfactory nerve fibres, Glia 52 (2005) 245–251.
[63] D. Tucker, Nonolfactory responses from the nasal cavity: Jacobson's organ and the trigeminal system, in: L.M. Beidler (Ed.), Handbook of Sensory Physiology, Springer, Berlin, 1971, pp. 151–181.
[64] K. Buchner, D. Seitz-Tutter, K. Schonitzer, D.G. Weiss, A quantitative study of anterograde and retrograde axonal transport of exogenous proteins in olfactory nerve C-fibers, Neuroscience 22 (1987) 697–707.
[65] J. Crank, The Mathematics of Diffusion, 2 ed. Oxford University Press, Oxford, 1975.
[66] R.G. Thorne, S. Hrabetova, C. Nicholson, Diffusion of epidermal growth factor in rat brain extracellular space measured by integrative optical imaging, J. Neurophysiol. 92 (2004) 3471–3481.
[67] T. Ichimura, P.A. Fraser, H.F. Cserr, Distribution of extracellular tracers in perivascular spaces of the rat brain, Brain Res. 545 (1991) 103–113.
[68] L.E. Bilston, D.F. Fletcher, A.R. Brodbelt, M.A. Stoodley, Arterial pulsation-driven cerebrospinal fluid flow in the perivascular space: a computational model, Comput. Methods Biomech. Biomed. Engin. 6 (2003) 235–241.
[69] D. Schley, R. Carare-Nnadi, C.P. Please, V.H. Perry, R.O. Weller, Mechanisms to explain the reverse perivascular transport of solutes out of the brain, J. Theor. Biol. 238 (2006) 962–974.
[70] P. Hadaczek, Y. Yamashita, H. Mirek, L. Tamas, M.C. Bohn, C. Noble, J.W. Park, K. Bankiewicz, The "perivascular pump" driven by arterial pulsation is a powerful mechanism for the distribution of therapeutic molecules within the brain, Mol. Ther. 14 (2006) 69–78.
[71] R.A. Scranton, L. Fletcher, S. Sprague, D.F. Jimenez, M. Digicaylioglu, The rostral migratory stream plays a key role in intranasal delivery of drugs into the CNS, PLoS One 6 (2011) e18711.
[72] L. Plum, M. Schubert, J.C. Bruning, The role of insulin receptor signaling in the brain, Trends Endocrinol. Metab. 16 (2005) 59–65.
[73] G.J. Francis, J.A. Martinez, W.Q. Liu, K. Xu, A. Ayer, J. Fine, U.I. Tuor, G. Glazner, L.R. Hanson, W.H. Frey II, C. Toth, Intranasal insulin prevents cognitive decline, cerebral atrophy and white matter changes in murine type I diabetic encephalopathy, Brain 131 (2008) 3311–3334.
[74] G. Francis, J. Martinez, W. Liu, T. Nguyen, A. Ayer, J. Fine, D. Zochodne, L.R. Hanson, W.H. Frey II, C. Toth, Intranasal insulin ameliorates experimental diabetic neuropathy, Diabetes 58 (2009) 934–945.
[75] D.R. Marks, K. Tucker, M.A. Cavallin, T.G. Mast, D.A. Fadool, Awake intranasal insulin delivery modifies protein complexes and alters memory, anxiety, and olfactory behaviors, J. Neurosci. 29 (2009) 6734–6751.
[76] M.J. During, L. Cao, D.S. Zuzga, J.S. Francis, H.L. Fitzsimons, X. Jiao, R.J. Bland, M. Klugmann, W.A. Banks, D.J. Drucker, C.N. Haile, Glucagon-like peptide-1 receptor is involved in learning and neuroprotection, Nat. Med. 9 (2003) 1173–1179.
[77] W.A. Banks, M.J. During, M.L. Niehoff, Brain uptake of the glucagon-like peptide-1 antagonist exendin(9–39) after intranasal administration, J. Pharmacol. Exp. Ther. 309 (2004) 469–475.
[78] R.G. Thorne, C. Nicholson, In vivo diffusion analysis with quantum dots and dextrans predicts the width of brain extracellular space, Proc. Natl. Acad. Sci. U.S.A. 103 (2006) 5567–5572.
[79] S.M. Krasnow, G.S. Fraley, S.M. Schuh, J.W. Baumgartner, D.K. Clifton, R.A. Steiner, A role for galanin-like peptide in the integration of feeding, body weight regulation, and reproduction in the mouse, Endocrinology 144 (2003) 813–822.
[80] N. Nonaka, S.A. Farr, H. Kageyama, S. Shioda, W.A. Banks, Delivery of galanin-like peptide to the brain: targeting with intranasal delivery and cyclodextrins, J. Pharmacol. Exp. Ther. 325 (2008) 513–519.
[81] S.A. Deadwyler, L. Porrino, J.M. Siegel, R.E. Hampson, Systemic and nasal delivery of orexin-A (Hypocretin-1) reduces the effects of sleep deprivation on cognitive performance in nonhuman primates, J. Neurosci. 27 (2007) 14239–14247.
[82] S.V. Dhuria, L.R. Hanson, W.H. Frey II, Intranasal drug targeting of hypocretin-1 (orexin-A) to the central nervous system, J. Pharm. Sci. 98 (2009) 2501–2515.
[83] I. Gozes, E. Giladi, A. Pinhasov, A. Bardea, D.E. Brenneman, Activity-dependent neurotrophic factor: intranasal administration of femtomolar-acting peptides improve performance in a water maze, J. Pharmacol. Exp. Ther. 293 (2000) 1091–1098.
[84] R.N. Alcalay, E. Giladi, C.G. Pick, I. Gozes, Intranasal administration of NAP, a neuroprotective peptide, decreases anxiety-like behavior in aging mice in the elevated plus maze, Neurosci. Lett. 361 (2004) 128–131.
[85] Y. Matsuoka, A.J. Gray, C. Hirata-Fukae, S.S. Minami, E.G. Waterhouse, M.P. Mattson, F.M. LaFerla, I. Gozes, P.S. Aisen, Intranasal NAP administration reduces accumulation of amyloid peptide and tau hyperphosphorylation in a transgenic mouse model of Alzheimer's disease at early pathological stage, J. Mol. Neurosci. 31 (2007) 165–170.
[86] N. Shiryaev, Y. Jouroukhin, E. Giladi, E. Polyzoidou, N.C. Grigoriadis, H. Rosenmann, I. Gozes, NAP protects memory, increases soluble tau and reduces tau hyperphosphorylation in a tauopathy model, Neurobiol. Dis. 34 (2009) 381–388.
[87] K.J. Powell, S.E. Hori, R. Leslie, A. Andrieux, H. Schellinck, M. Thorne, G.S. Robertson, Cognitive impairments in the STOP null mouse model of schizophrenia, Behav. Neurosci. 121 (2007) 826–835.
[88] N.K. Sharma, N.K. Sethy, R.N. Meena, G. Ilavazhagan, M. Das, K. Bhargava, Activity-dependent neuroprotective protein (ADNP)-derived peptide (NAP) ameliorates hypobaric hypoxia induced oxidative stress in rat brain, Peptides, 2011.
[89] B.L. Sun, F.P. Shen, Q.J. Wu, S.M. Chi, M.F. Yang, H. Yuan, F.M. Xie, Y.B. Zhang, J. Chen, F. Zhang, Intranasal delivery of calcitonin gene-related peptide reduces cerebral vasospasm in rats, Front. Biosci. (Elite Ed.) 2 (2010) 1502–1513.
[90] D. Rat, U. Schmitt, F. Tippmann, I. Dewachter, C. Theunis, E. Wieczerzak, R. Postina, F. van Leuven, F. Fahrenholz, E. Kojro, Neuropeptide pituitary adenylate cyclase-activating polypeptide (PACAP) slows down Alzheimer's disease-like pathology in amyloid precursor protein-transgenic mice, FASEB J. 25 (2011) 3208–3218.
[91] X.F. Liu, J.R. Fawcett, R.G. Thorne, T.A. DeFor, W.H. Frey II, Intranasal administration of insulin-like growth factor-I bypasses the blood–brain barrier and protects against focal cerebral ischemic damage, J. Neurol. Sci. 187 (2001) 91–97.
[92] X.F. Liu, J.R. Fawcett, R.G. Thorne, W.H. Frey II, Non-invasive intranasal insulin-like growth factor-I reduces infarct volume and improves neurologic function in rats following middle cerebral artery occlusion, Neurosci. Lett. 308 (2001) 91–94.
[93] X.F. Liu, J.R. Fawcett, L.R. Hanson, W.H. Frey II, The window of opportunity for treatment of focal cerebral ischemic damage with noninvasive intranasal insulin-like growth factor-I in rats, J. Stroke Cerebrovasc. Dis. 13 (2004) 16–23.
[94] S. Lin, L.W. Fan, P.G. Rhodes, Z. Cai, Intranasal administration of IGF-1 attenuates hypoxic–ischemic brain injury in neonatal rats, Exp. Neurol. 217 (2009) 361–370.
[95] G. Grasso, A. Sfacteria, F. Meli, M. Passalacqua, V. Fodale, M. Buemi, F. Giambartino, D.G. Iacopino, F. Tomasello, The role of erythropoietin in neuroprotection: therapeutic perspectives, Drug News Perspect. 20 (2007) 315–320.
[96] Y.P. Yu, Q.Q. Xu, Q. Zhang, W.P. Zhang, L.H. Zhang, E.Q. Wei, Intranasal recombinant human erythropoietin protects rats against focal cerebral ischemia, Neurosci. Lett. 387 (2005) 5–10.
[97] L. Fletcher, S. Kohli, S.M. Sprague, R.A. Scranton, S.A. Lipton, A. Parra, D.F. Jimenez, M. Digicaylioglu, Intranasal delivery of erythropoietin plus insulin-like growth factor-I for acute neuroprotection in stroke. Laboratory investigation, J. Neurosurg. 111 (2009) 164–170.
[98] Y.J. Kang, M. Digicaylioglu, R. Russo, M. Kaul, C.L. Achim, L. Fletcher, E. Masliah, S.A. Lipton, Erythropoietin plus insulin-like growth factor-I protects against neuronal damage in a murine model of human immunodeficiency virus-associated neurocognitive disorders, Ann. Neurol. 68 (2010) 342–352.
[99] S.R. Alcala-Barraza, M.S. Lee, L.R. Hanson, A.A. McDonald, W.H. Frey 2nd, L.K. McLoon, Intranasal delivery of neurotrophic factors BDNF, CNTF, EPO, and NT-4 to the CNS, J. Drug Target. 18 (2010) 179–190.
[100] T.M. Ross, P.M. Martinez, J.C. Renner, R.G. Thorne, L.R. Hanson, W.H. Frey 2nd, Intranasal administration of interferon beta bypasses the blood–brain barrier to target the central nervous system and cervical lymph nodes: a non-invasive treatment strategy for multiple sclerosis, J. Neuroimmunol. 151 (2004) 66–77.
[101] M.M. Migliore, T.K. Vyas, R.B. Campbell, M.M. Amiji, B.L. Waszczak, Brain delivery of proteins by the intranasal route of administration: a comparison of cationic liposomes versus aqueous solution formulations, J. Pharm. Sci. 99 (2010) 1745–1761.
[102] W.A. Banks, C.L. Farrell, Impaired transport of leptin across the blood–brain barrier in obesity is acquired and reversible, Am. J. Physiol. Endocrinol. Metab. 285 (2003) E10–E15.
[103] S. Fliedner, C. Schulz, H. Lehnert, Brain uptake of intranasally applied radioiodinated leptin in Wistar rats, Endocrinology 147 (2006) 2088–2094.
[104] C. Schulz, K. Paulus, H. Lehnert, Central nervous and metabolic effects of intranasally applied leptin, Endocrinology 145 (2004) 2696–2701.
[105] H. Shimizu, I.S. Oh, S. Okada, M. Mori, Inhibition of appetite by nasal leptin administration in rats, Int. J. Obes. (Lond) 29 (2005) 858–863.
[106] L. Xu, N. Rensing, X.F. Yang, H.X. Zhang, L.L. Thio, S.M. Rothman, A.E. Weisenfeld, M. Wong, K.A. Yamada, Leptin inhibits 4-aminopyridine- and pentylenetetrazole-

induced seizures and AMPAR-mediated synaptic transmission in rodents, J. Clin. Invest. 118 (2008) 272–280.
[107] X.Q. Chen, J.R. Fawcett, Y.E. Rahman, T.A. Ala, I.W. Frey, Delivery of nerve growth factor to the brain via the olfactory pathway, J. Alzheimers Dis. 1 (1998) 35–44.
[108] S. Capsoni, S. Giannotta, A. Cattaneo, Nerve growth factor and galantamine ameliorate early signs of neurodegeneration in anti-nerve growth factor mice, Proc. Natl. Acad. Sci. U.S.A. 99 (2002) 12432–12437.
[109] R. De Rosa, A.A. Garcia, C. Braschi, S. Capsoni, L. Maffei, N. Berardi, A. Cattaneo, Intranasal administration of nerve growth factor (NGF) rescues recognition memory deficits in AD11 anti-NGF transgenic mice, Proc. Natl. Acad. Sci. U.S.A. 102 (2005) 3811–3816.
[110] C.G. Shi, L.M. Wang, Y. Wu, P. Wang, Z.J. Gan, K. Lin, L.X. Jiang, Z.Q. Xu, M. Fan, Intranasal administration of nerve growth factor produces antidepressant-like effects in animals, Neurochem. Res. 35 (2010) 1302–1314.
[111] W. Zhu, S. Cheng, G. Xu, M. Ma, Z. Zhou, D. Liu, X. Liu, Intranasal nerve growth factor enhances striatal neurogenesis in adult rats with focal cerebral ischemia, Drug Deliv. 18 (2011) 338–343.
[112] J.P. Yang, H.J. Liu, S.M. Cheng, Z.L. Wang, X. Cheng, H.X. Yu, X.F. Liu, Direct transport of VEGF from the nasal cavity to brain, Neurosci. Lett. 449 (2009) 108–111.
[113] J.P. Yang, H.J. Liu, Z.L. Wang, S.M. Cheng, X. Cheng, G.L. Xu, X.F. Liu, The dose-effectiveness of intranasal VEGF in treatment of experimental stroke, Neurosci. Lett. 461 (2009) 212–216.
[114] Y.P. Ma, M.M. Ma, S. Ge, R.B. Guo, H.J. Zhang, W.H. Frey 2nd, G.L. Xu, X.F. Liu, Intranasally delivered TGF-beta1 enters brain and regulates gene expressions of its receptors in rats, Brain Res. Bull. 74 (2007) 271–277.
[115] M. Ma, Y. Ma, X. Yi, R. Guo, W. Zhu, X. Fan, G. Xu, W.H. Frey 2nd, X. Liu, Intranasal delivery of transforming growth factor-beta1 in mice after stroke reduces infarct volume and increases neurogenesis in the subventricular zone, BMC Neurosci. 9 (2008) 117.
[116] Y.P. Ma, M.M. Ma, S.M. Cheng, H.H. Ma, X.M. Yi, G.L. Xu, X.F. Liu, Intranasal bFGF-induced progenitor cell proliferation and neuroprotection after transient focal cerebral ischemia, Neurosci. Lett. 437 (2008) 93–97.
[117] Z.L. Wang, S.M. Cheng, M.M. Ma, Y.P. Ma, J.P. Yang, G.L. Xu, X.F. Liu, Intranasally delivered bFGF enhances neurogenesis in adult rats following cerebral ischemia, Neurosci. Lett. 446 (2008) 30–35.
[118] W.A. Banks, Are the extracellular pathways a conduit for the delivery of therapeutics to the brain? Curr. Pharm. Des. 10 (2004) 1365–1370.
[119] E. Furrer, V. Hulmann, D.M. Urech, Intranasal delivery of ESBA105, a TNF-alpha-inhibitory scFv antibody fragment to the brain, J. Neuroimmunol. 215 (2009) 65–72.
[120] S. Cattepoel, M. Hanenberg, L. Kulic, R.M. Nitsch, Chronic intranasal treatment with an anti-abeta(30–42) scFv antibody ameliorates amyloid pathology in a transgenic mouse model of Alzheimer's disease, PLoS One 6 (2011) e18296.
[121] V.Y. Gorbatov, N.A. Trekova, V.G. Fomina, T.V. Davydova, Antiamnestic effects of antibodies to glutamate in experimental Alzheimer's disease, Bull. Exp. Biol. Med. 150 (2010) 23–25.
[122] G.A. Romanova, F.M. Shakova, V.Y. Gorbatov, Y.N. Kvashennikova, T.V. Davydova, Effect of antibodies to glutamate on retention of conditioned passive avoidance response in rats with ischemic injury of the prefrontal cortex, Bull. Exp. Biol. Med. 149 (2010) 289–292.
[123] R. Draghia, C. Caillaud, R. Manicom, A. Pavirani, A. Kahn, L. Poenaru, Gene delivery into the central nervous system by nasal instillation in rats, Gene Ther. 2 (1995) 418–423.
[124] Y.K. Oh, J.P. Kim, T.S. Hwang, J.J. Ko, J.M. Kim, J.S. Yang, C.K. Kim, Nasal absorption and biodistribution of plasmid DNA: an alternative route of DNA vaccine delivery, Vaccine 19 (2001) 4519–4525.
[125] I.K. Han, M.Y. Kim, H.M. Byun, T.S. Hwang, J.M. Kim, K.W. Hwang, T.G. Park, W.W. Jung, T. Chun, G.J. Jeong, Y.K. Oh, Enhanced brain targeting efficiency of intranasally administered plasmid DNA: an alternative route for brain gene therapy, J. Mol. Med. 85 (2007) 75–83.
[126] J.M. Laing, M.D. Gober, E.K. Golembewski, S.M. Thompson, K.A. Gyure, P.J. Yarowsky, L. Aurelian, Intranasal administration of the growth-compromised HSV-2 vector DeltaRR prevents kainate-induced seizures and neuronal loss in rats and mice, Mol. Ther. 13 (2006) 870–881.
[127] I.S. Rakover, N. Zabavnik, R. Kopel, M. Paz-Rozner, B. Solomon, Antigen-specific therapy of EAE via intranasal delivery of filamentous phage displaying a myelin immunodominant epitope, J. Neuroimmunol. 225 (2010) 68–76.
[128] D. Frenkel, B. Solomon, Filamentous phage as vector-mediated antibody delivery to the brain, Proc. Natl. Acad. Sci. U.S.A. 99 (2002) 5675–5679.
[129] I.D. Kim, S.W. Kim, J.K. Lee, Gene knockdown in the olfactory bulb, amygdala, and hypothalamus by intranasal siRNA administration, Korean J. Anat. 42 (2009) 285–292.
[130] L. Danielyan, R. Schafer, A. von Ameln-Mayerhofer, M. Buadze, J. Geisler, T. Klopfer, U. Burkhardt, B. Proksch, S. Verleysdonk, M. Ayturan, G.H. Buniatian, C.H. Gleiter, W.H. Frey 2nd, Intranasal delivery of cells to the brain, Eur. J. Cell Biol. 88 (2009) 315–324.
[131] L. Danielyan, R. Schafer, A. von Ameln-Mayerhofer, F. Bernhard, S. Verleysdonk, M. Buadze, A. Lourhmati, T. Klopfer, F. Schaumann, B. Schmid, C. Koehle, B. Proksch, R. Weissert, H.M. Reichardt, J. van den Brandt, G.H. Buniatian, M. Schwab, C.H. Gleiter, W.H. Frey II, Therapeutic efficacy of intranasally delivered mesenchymal stem cells in a rat model of Parkinson disease, Rejuvenation Res. 14 (2011) 3–16.
[132] C.T. van Velthoven, A. Kavelaars, F. van Bel, C.J. Heijnen, Nasal administration of stem cells: a promising novel route to treat neonatal ischemic brain damage, Pediatr. Res. 68 (2010) 419–422.
[133] R. Pietrowsky, C. Struben, M. Molle, H.L. Fehm, J. Born, Brain potential changes after intranasal vs. intravenous administration of vasopressin: evidence for a direct nose–brain pathway for peptide effects in humans, Biol. Psychiatry 39 (1996) 332–340.
[134] R. Pietrowsky, A. Thiemann, W. Kern, H.L. Fehm, J. Born, A nose–brain pathway for psychotropic peptides: evidence from a brain evoked potential study with cholecystokinin, Psychoneuroendocrinology 21 (1996) 559–572.
[135] I. Derad, K. Willeke, R. Pietrowsky, J. Born, H.L. Fehm, Intranasal angiotensin II directly influences central nervous regulation of blood pressure, Am. J. Hypertens. 11 (1998) 971–977.
[136] J. Culman, J. Baulmann, A. Blume, T. Unger, The renin–angiotensin system in the brain: an update, J. Renin Angiotensin Aldosterone Syst. 2 (2001) 96–102.
[137] J. Born, T. Lange, W. Kern, G.P. McGregor, U. Bickel, H.L. Fehm, Sniffing neuropeptides: a transnasal approach to the human brain, Nat. Neurosci. 5 (2002) 514–516.
[138] H.L. Fehm, R. Smolnik, W. Kern, G.P. McGregor, U. Bickel, J. Born, The melanocortin melanocyte-stimulating hormone/adrenocorticotropin(4–10) decreases body fat in humans, J. Clin. Endocrinol. Metabol. 86 (2001) 1144–1148.
[139] R. Smolnik, B. Perras, M. Molle, H.L. Fehm, J. Born, Event-related brain potentials and working memory function in healthy humans after single-dose and prolonged intranasal administration of adrenocorticotropin 4–10 and desacetyl-alpha-melanocyte stimulating hormone, J. Clin. Psychopharmacol. 20 (2000) 445–454.
[140] M. Hallschmid, R. Smolnik, G. McGregor, J. Born, H.L. Fehm, Overweight humans are resistant to the weight-reducing effects of melanocortin4–10, J. Clin. Endocrinol. Metabol. 91 (2006) 522–525.
[141] W. Kern, J. Born, H. Schreiber, H.L. Fehm, Central nervous system effects of intranasally administered insulin during euglycemia in men, Diabetes 48 (1999) 557–563.
[142] C. Benedict, M. Hallschmid, A. Hatke, B. Schultes, H.L. Fehm, J. Born, W. Kern, Intranasal insulin improves memory in humans, Psychoneuroendocrinology 29 (2004) 1326–1334.
[143] C. Benedict, W. Kern, B. Schultes, J. Born, M. Hallschmid, Differential sensitivity of men and women to anorexigenic and memory-improving effects of intranasal insulin, J. Clin. Endocrinol. Metab. 93 (2008) 1339–1344.
[144] C. Benedict, S. Brede, H.B. Schioth, H. Lehnert, B. Schultes, J. Born, M. Hallschmid, Intranasal insulin enhances postprandial thermogenesis and lowers postprandial serum insulin levels in healthy men, Diabetes 60 (2011) 114–118.
[145] M.A. Reger, G.S. Watson, P.S. Green, C.W. Wilkinson, L.D. Baker, B. Cholerton, M.A. Fishel, S.R. Plymate, J.C. Breitner, W. DeGroodt, P. Mehta, S. Craft, Intranasal insulin improves cognition and modulates beta-amyloid in early AD, Neurology 70 (2008) 440–448.
[146] A. Ermisch, T. Barth, H.J. Ruhle, J. Skopkova, P. Hrbas, R. Landgraf, On the blood–brain barrier to peptides: accumulation of labelled vasopressin, DesGlyNH2-vasopressin and oxytocin by brain regions, Endocrinol. Exp. 19 (1985) 29–37.
[147] Y.S. Kang, J.H. Park, Brain uptake and the analgesic effect of oxytocin—its usefulness as an analgesic agent, Arch. Pharm. Res. 23 (2000) 391–395.
[148] M. Kosfeld, M. Heinrichs, P.J. Zak, U. Fischbacher, E. Fehr, Oxytocin increases trust in humans, Nature 435 (2005) 673–676.
[149] P. Kirsch, C. Esslinger, Q. Chen, D. Mier, S. Lis, S. Siddhanti, H. Gruppe, V.S. Mattay, B. Gallhofer, A. Meyer-Lindenberg, Oxytocin modulates neural circuitry for social cognition and fear in humans, J. Neurosci. 25 (2005) 11489–11493.
[150] G. Domes, M. Heinrichs, A. Michel, C. Berger, S.C. Herpertz, Oxytocin improves “mind-reading” in humans, Biol. Psychiatry 61 (2007) 731–733.
[151] M. Heinrichs, T. Baumgartner, C. Kirschbaum, U. Ehlert, Social support and oxytocin interact to suppress cortisol and subjective responses to psychosocial stress, Biol. Psychiatry 54 (2003) 1389–1398.
[152] I. Labuschagne, K.L. Phan, A. Wood, M. Angstadt, P. Chua, M. Heinrichs, J.C. Stout, P.J. Nathan, Oxytocin attenuates amygdala reactivity to fear in generalized social anxiety disorder, Neuropsychopharmacology 35 (2010) 2403–2413.
[153] A.J. Guastella, S.L. Einfeld, K.M. Gray, N.J. Rinehart, B.J. Tonge, T.J. Lambert, I.B. Hickie, Intranasal oxytocin improves emotion recognition for youth with autism spectrum disorders, Biol. Psychiatry 67 (2010) 692–694.
[154] K. Macdonald, T.M. Macdonald, The peptide that binds: a systematic review of oxytocin and its prosocial effects in humans, Harv. Rev. Psychiatry 18 (2010) 1–21.
[155] A. Meyer-Lindenberg, G. Domes, P. Kirsch, M. Heinrichs, Oxytocin and vasopressin in the human brain: social neuropeptides for translational medicine, Nat. Rev. Neurosci. 12 (2011) 524–538.
[156] J.R. Harkema, Comparative pathology of the nasal mucosa in laboratory animals exposed to inhaled irritants, Environ. Health Perspect. 85 (1990) 231–238.
[157] J.P. Schreider, Comparative anatomy and function of the nasal passages, in: C.S. Barrow (Ed.), Toxicology of the Nasal Passages, Hemisphere, New York, 1986.